Research Square

Preprints are preliminary reports that have not undergone peer review.
They should not be considered conclusive, used to inform clinical practice,
or referenced by the media as validated information.

Integrated Geophysical Assessment of Aquifer Geometry and Groundwater Potential in a Basement Complex Terrain, Southwestern Nigeria: Combining Vertical Electrical Sounding, Self-Potential, and Pumping Tests

Solomon M. Jekayinfa[1]

solomon.jekayinfa@uniosun.edu.ng

Osun State University

Rasaq A. Azeez[1]

Osun State University

Olabanji A. Ojo[1]

Osun State University

Article

Keywords: Vertical electrical sounding, Self-potential, Aquifer geometry, Groundwater potential, Basement complex, Nigeria

Posted Date: July 20th, 2026

DOI: https://doi.org/10.21203/rs.3.rs-10218064/v1

License: This work is licensed under a Creative Commons Attribution 4.0 International License.
Read Full License

Additional Declarations: No competing interests reported.

INTEGRATED GEOPHYSICAL ASSESSMENT OF AQUIFER GEOMETRY AND GROUNDWATER POTENTIAL IN A BASEMENT COMPLEX TERRAIN, SOUTHWESTERN NIGERIA: COMBINING VERTICAL ELECTRICAL SOUNDING, SELF-POTENTIAL, AND PUMPING TESTS.

Solomon M. Jekayinfa[1], Rasaq A. Azeez[1], Olabanji A. Ojo[1]

[1]Department of Geological Sciences, Osun State University, Osogbo, Nigeria

Corresponding author: solomon.jekayinfa@uniosun.edu.ng

ABSTRACT

Groundwater occurrence in crystalline basement terrains is restricted to secondary porosity features such as weathered zones and fractures, making exploration challenging. This study presents an integrated geophysical assessment of aquifer geometry and groundwater potential within the basement complex terrain of Osun State University campus, Osogbo, Southwestern Nigeria. Six Vertical Electrical Sounding (VES) surveys using the Schlumberger array (AB/2 = 1-100 m), six Self-Potential (SP) profiles (100-m traverses), and constant-rate pumping tests (120 minutes; 36.7-45.2 L/min) were conducted. VES data were inverted using iterative optimization (RMS < 5%), and SP data were analyzed to identify groundwater flow anomalies. Results revealed 3-4 geoelectric layers: topsoil, lateritic clay, weathered basement (aquifer zone, 3.8-23.3 m thick, 30-171 Ωm), and fresh/fractured basement. The highest groundwater potential occurred at the Engineering Building (VES 4) with a thick, low-resistivity saturated weathered layer (15.7 m, 30 Ωm) underlain by fractured basement (418 Ωm), and a very strong SP anomaly (+700 mV). SP anomalies ranged from -180 to +700 mV. Aquifer tests revealed specific capacities of 6.02-7.93 L/min/m and transmissivity of 9.4-12.4 m²/day. A strong positive correlation ($r = 0.71$, $p < 0.05$) between SP anomaly magnitude and specific capacity confirms that SP responses reflect active groundwater movement rather than merely saturated conditions. The integrated VES-SP approach proved more reliable than either method alone, as VES delineated storage capacity while SP identified permeability. This study provides a cost-effective framework for groundwater exploration in crystalline basement terrains, demonstrating that targeting zones with thick, low-resistivity weathered layers and strong positive SP anomalies significantly improves borehole siting success rates.

Keywords: Vertical electrical sounding · Self-potential · Aquifer geometry · Groundwater potential · Basement complex · Nigeria

1. INTRODUCTION

Groundwater constitutes the most reliable freshwater source in tropical crystalline basement terrains, particularly in developing countries where surface water resources are increasingly compromised by seasonal variability and anthropogenic pollution (Todd and Mays 2005; MacDonald et al. 2012). In Nigeria, over 60% of the population depends on groundwater for domestic, agricultural, and industrial needs, with basement complex aquifers serving as primary

sources across southwestern regions (Olorunfemi and Fasuyi 1993; Adelana et al. 2008). The increasing water demand driven by population growth, urbanization, and climate variability has intensified pressure on these groundwater resources, necessitating improved exploration and management strategies (Aizebeokhai 2010; Bayowa et al. 2023).

Crystalline basement terrains, covering approximately 50% of Nigeria's landmass, present unique hydrogeological challenges due to their negligible primary porosity (Rahaman 1988; Wright 1992). Groundwater occurrence in these terrains is restricted to secondary porosity features such as weathered zones, fractures, joints, and faults, which are often discontinuous and heterogeneous (Omosuyi et al. 2007; Adiat et al. 2009). The weathered regolith (saprolite) provides storage capacity, while fracture networks facilitate groundwater flow and determine borehole yield (MacDonald et al. 2005). Successful groundwater development in such complex geological settings, therefore, depends critically on the accurate delineation of these secondary porosity zones, which serve as the primary pathways for groundwater storage and flow (Olorunfemi and Ojo 2003; Gemail et al. 2020).

Geophysical methods have proven indispensable for subsurface characterization in basement terrains. The Vertical Electrical Sounding (VES) method enables the delineation of subsurface layers based on resistivity contrast, which depends on lithology, moisture content, and degree of saturation (Telford et al. 1990; Loke and Barker 1996). VES can identify weathered and fractured zones that constitute potential aquifers, with numerous studies demonstrating its effectiveness in basement terrains across West Africa (Olorunfemi and Fasuyi 1993; Olayinka and Olorunfemi 1992; Adiat et al. 2009; Akinlalu et al. 2017). However, resistivity alone cannot distinguish between stored water (storage capacity) and flowing water (permeability), a critical limitation for predicting borehole yield.

The Self-Potential (SP) method complements VES by detecting naturally occurring voltage differences generated by electrokinetic potentials associated with groundwater flow through porous media and fractures (Revil et al. 2003; Soupios et al. 2007). Positive SP anomalies typically indicate zones of active groundwater movement, while negative or flat anomalies suggest limited flow or clay-rich, low-permeability zones (Corwin and Hoover 1979; Jouniaux et al. 2000). Recent advances in SP interpretation have improved our understanding of the relationship between SP signals and hydraulic parameters (Revil and Ghorbani 2025; Maineult et al. 2006). The integration of SP with electrical methods has proven particularly effective for characterizing groundwater flow paths in structurally complex environments (El-Qady et al. 2016; Gemail et al. 2020; Rittgers et al. 2013).

Several studies have applied integrated geophysical approaches for groundwater exploration in Nigerian basement terrains. Omosuyi et al. (2007) combined VES and electromagnetic methods in Ondo State, while Adiat et al. (2009) used VES and pumping tests to evaluate groundwater potential in Igbara-Odo. Bayowa et al. (2023) applied 2D resistivity imaging for aquifer characterization in Osogbo. However, within the Osun State University (UNIOSUN) campus, previous geophysical studies were conducted independently without integration with aquifer yield data, and no comprehensive assessment of groundwater potential has been undertaken. This

knowledge gap limits informed decision-making for borehole siting and water resource management on the campus.

The specific objectives of this study are: (1) to delineate subsurface geoelectric layers and identify potential aquifer zones using VES; (2) to identify active groundwater flow zones using SP surveys; (3) to assess aquifer yield parameters through constant-rate pumping tests; and (4) to establish empirical correlations between geophysical parameters (resistivity, SP anomalies) and hydraulic parameters (specific capacity, transmissivity). The novelty of this study lies in the systematic integration of VES, SP, and pumping test data to characterize both storage capacity and permeability, providing a replicable framework for groundwater exploration in similar basement terrains across West Africa and other tropical regions.

2. STUDY AREA

2.1 Location and Physiography

The study area is located within the main campus of Osun State University (UNIOSUN), Osogbo, Osun State, Southwestern Nigeria (Fig. 1). It lies between latitudes 7°45′N and 7°50′N and longitudes 4°30′E and 4°37′E, covering approximately 2 km². The area is accessible via the Osogbo-Ibadan and Osogbo-Ede highways, making it suitable for long-term monitoring studies.

The climate is humid tropical, characterized by distinct wet (April-October) and dry (November-March) seasons, governed by the movement of the Intertropical Convergence Zone (ITCZ). Mean annual rainfall ranges from 1,200 to 1,400 mm, with a double maximum in July and September (NIMET 2023). The rainfall pattern is typical of the equatorial rainforest zone, with high-intensity storms contributing significantly to groundwater recharge. Temperatures average 27°C, with a range of 25-32°C, and relative humidity varies between 60% and 85% (NIMET 2023). The dominant vegetation is derived savannah, characterized by scattered trees, shrubs, and grasses, with remnants of tropical rainforest in protected areas.

Topographically, the area is gently undulating, with elevations ranging from 300 to 360 m above sea level. Drainage is primarily controlled by the Oshun River and its tributaries, which flow in a general southward direction. The relatively low relief and moderate slopes facilitate infiltration and groundwater recharge.

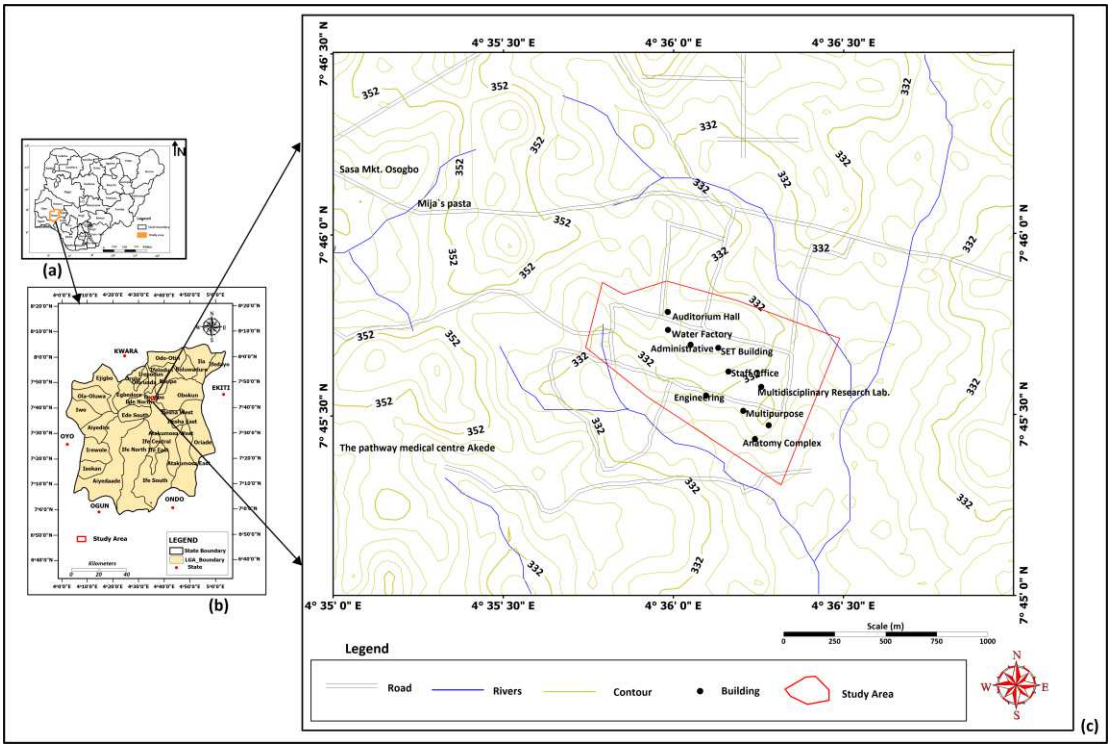


Figure 1: Location Map of the Study Area (culled from Topographical Map of Ilesha NW Sheet 243 1: 50 000 (1965)), the inset is the administrative map of Osun state showing the study area and the Nigeria map.

2.2 Geological Setting

Osogbo lies within the Precambrian Basement Complex of Southwestern Nigeria, which forms part of the Pan-African mobile belt (600-450 Ma) (Rahaman 1988; Olorunfemi and Ojo 2003). The Basement Complex comprises three major lithological groups: the migmatite-gneiss-quartzite complex, the schist belts, and the older granites (Rahaman 1988). The study area falls within the schist belt, which consists of metasedimentary and metavolcanic rocks that have undergone polyphase deformation and metamorphism (Odeyemi 1993).

The dominant lithological unit around the UNIOSUN campus is amphibolite schist (Fig. 2), characterized by its foliated texture and composed primarily of amphibole minerals (hornblende) with plagioclase feldspar, garnet, and accessory minerals (Bayowa et al. 2023). The amphibolite schist is part of the Ilesha Schist Belt, which extends northeast-southwest across Osun and Ondo states (Rahaman 1988). The weathered products of the amphibolite schist give rise to the clayey to sandy clay overburden observed across the campus, with the degree of weathering varying considerably due to differences in fracture density, mineralogy, and topographic position.

The structural framework of the area is characterized by two dominant fracture orientations: northeast-southwest (NNE-SSW) and northwest-southeast (NW-SE), which are consistent with the regional Pan-African structural trends (Odeyemi 1993; Oluyide 1988). These fractures serve as the

primary conduits for groundwater flow, with their intersections often forming zones of enhanced permeability. The weathering profile developed on the amphibolite schist typically exhibits four zones: (1) a thin topsoil zone (0.5-2.0 m); (2) a lateritic clay zone (2-10 m); (3) a weathered basement or saprolite zone (5-25 m); and (4) fresh to partially fractured bedrock (Olorunfemi and Ojo 2003; Bayowa et al. 2023).

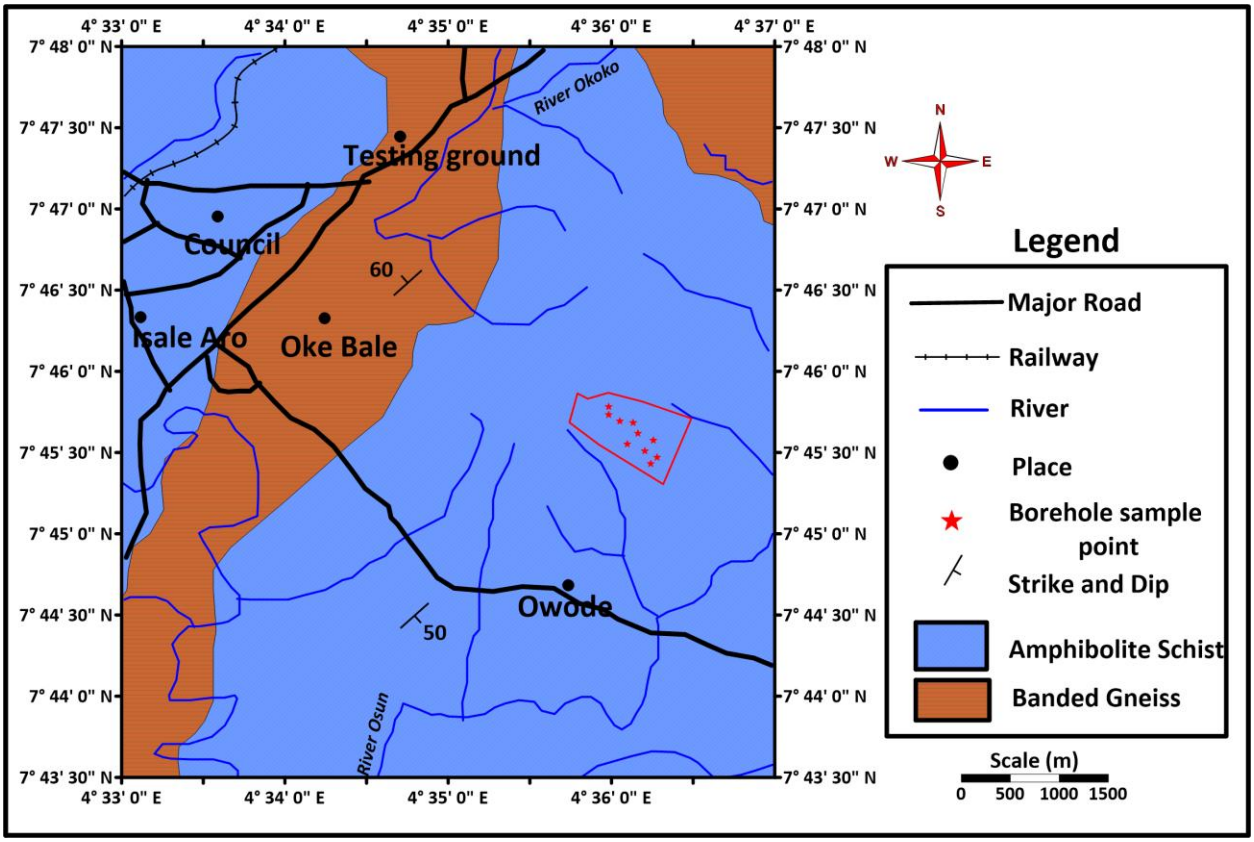


Figure 2: Geological map of the study area, culled from the *Geological Map of Osogbo Area (after Bayowa et. al., 2023)*

2.3 Hydrogeological Setting

The hydrogeological regime of the study area consists of two distinct aquifer systems, which is typical of crystalline basement terrains in West Africa (Wright 1992; MacDonald et al. 2005):

1. **Shallow unconfined aquifer**: This aquifer occurs within the weathered regolith (saprolite) and is typically 5-25 m thick. It consists of clayey sand to sandy clay derived from the in-situ weathering of the underlying amphibolite schist. This horizon provides storage capacity through intergranular porosity, with hydraulic conductivity varying from 10^{-5} to 10^{-3} m/s depending on the clay content and degree of weathering (Olorunfemi and Ojo 2003). The water table in this aquifer is generally shallow (5-10 m below ground surface) and exhibits seasonal fluctuations of 2-5 m in response to rainfall variability.

2. **Deeper semi-confined aquifer**: This aquifer occurs within fractures and joints in the bedrock at depths of 30-60 m (Olorunfemi and Ojo 2003). Fracture density and

connectivity control the permeability of this aquifer, with hydraulic conductivity typically ranging from 10^{-6} to 10^{-4} m/s (MacDonald et al. 2005). The fracture networks are often interconnected, facilitating groundwater flow over considerable distances. This aquifer provides the main source for borehole water supply in the area, as it is less susceptible to seasonal fluctuations and contamination than the shallow aquifer.

Recharge to the aquifer system occurs primarily through direct rainfall infiltration, with recharge rates estimated at 5-15% of annual precipitation (Adelana et al. 2008; Okogbue and Aghamelu 2010). The recharge process is facilitated by the permeable nature of the topsoil and the presence of fractures that allow rapid infiltration during high-intensity rainfall events. Groundwater flow is generally towards the Oshin River, with flow directions influenced by the topography and fracture orientations (Bayowa et al. 2023). Groundwater quality in the area is generally good, with electrical conductivity values ranging from 50 to 300 μS/cm and major ion concentrations within acceptable limits for drinking water (Olorunfemi and Ojo 2003).

3. MATERIALS AND METHODS

3.1 VES Survey Design and Data Acquisition

Vertical Electrical Sounding (VES) surveys were conducted at six locations corresponding to existing borehole points distributed across the UNIOSUN campus: Multipurpose Complex, Multidisciplinary Research Building, Anatomy Complex, Engineering Building, Behind ATM Stand (SET Building), and Staff Office (Fig. 1). The ABEM SAS 1000 Terrameter was employed for all electrical measurements, with the instrument calibrated before each survey to ensure data quality.

VES surveys utilized the Schlumberger electrode array configuration with half-current electrode spacing (AB/2) ranging from 1 to 100 m (Telford et al. 1990). The Schlumberger array was selected due to its enhanced sensitivity to horizontal layer boundaries, making it particularly suitable for characterizing the layered weathered profiles typical of basement terrains. The electrode configuration consists of two outer current electrodes (A and B) and two inner potential electrodes (M and N), with the potential electrodes maintained at a fixed spacing (MN = 2-5 m) while the current electrode spacing is systematically increased (Fig. 3). The apparent resistivity (ρa) was calculated from the measured potential difference (ΔV) and injected current (I) using the geometric factor appropriate for the Schlumberger array:

$$\rho a = K * (\Delta V/I)$$

where $K = [\pi(AB/2)^2 - (MN/2)^2]/(2*MN)$

Data quality was ensured by taking duplicate measurements at each electrode spacing and monitoring the consistency of readings. Electrode contact resistances were maintained below 1000 Ωm by pouring saline water at electrode positions where necessary, as recommended by Telford et al. (1990). The maximum current electrode spacing (AB/2 = 100 m) provided investigation depths

of approximately 60-80 m, sufficient to characterize the entire weathering profile and the underlying basement.

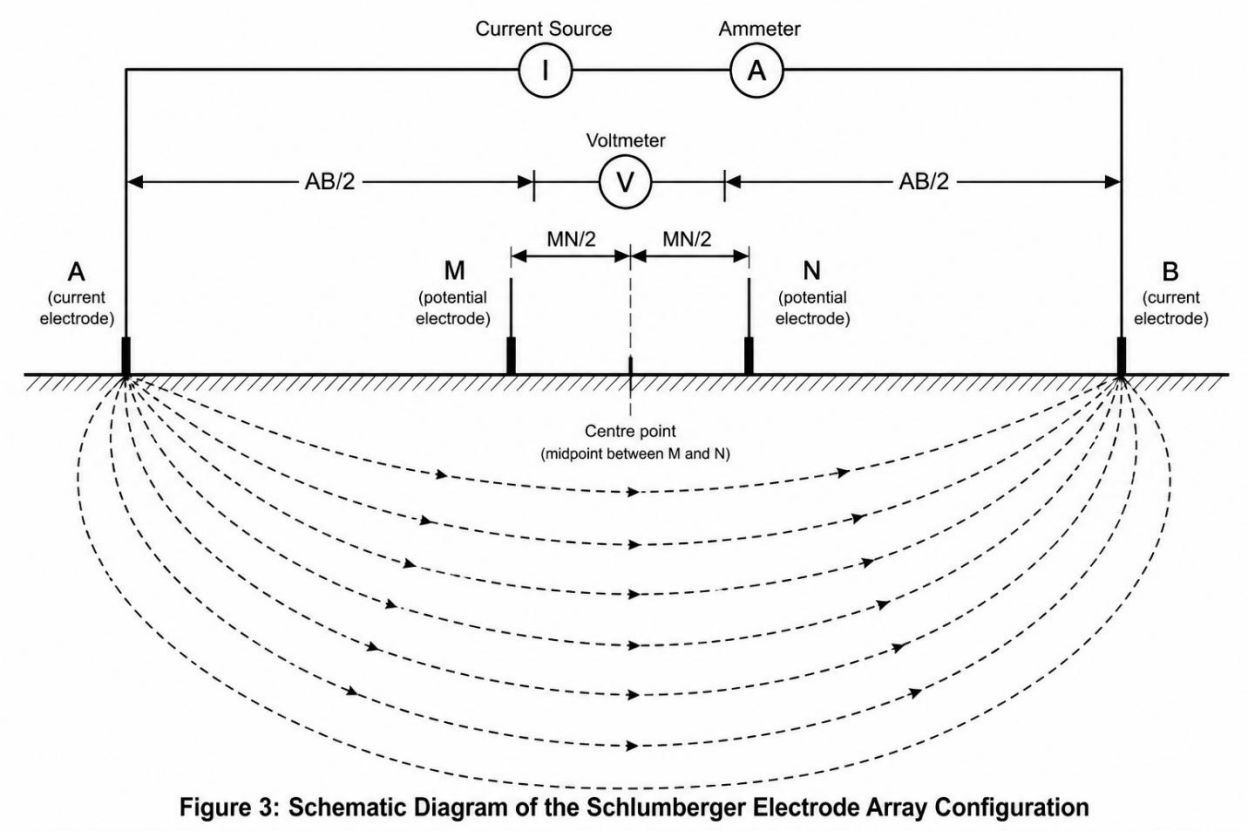


Figure 3: Schematic Diagram of the Schlumberger Electrode Array Configuration

Figure 3: Schematic Diagram of the Schlumberger Electrode Array Configuration

3.2 VES Data Processing and Inversion

The field resistivity data were processed using an iterative optimization algorithm implemented in RESIST software (Vander Velpen 1988). The inversion process minimizes the root-mean-square (RMS) error between the measured and calculated apparent resistivity values, progressively refining the layer parameters (resistivity and thickness) until an optimal fit is achieved. The inversion employs the Marquardt-Levenberg algorithm, which combines the steepest descent and Gauss-Newton methods for efficient convergence (Marquardt 1963).

Initial models for the inversion were derived from the qualitative interpretation of the sounding curves, with the number of layers determined by the shape of the field curves (Orellana and Mooney 1966; Zohdy 1974). A model fit with RMS error below 5% was obtained for all VES stations, indicating a high degree of data-model consistency and reliable layer parameter estimates. The reliability of the inverted parameters was assessed by analyzing the equivalence and suppression effects inherent in resistivity sounding interpretation (Koefoed 1979). For each VES station, the curve type was classified according to the sequence of layer resistivities following the standard nomenclature (Orellana and Mooney 1966; Zohdy 1974). The final geoelectric models

were constrained by borehole lithological logs where available, improving the accuracy of lithological interpretation.

Recent studies have demonstrated the effectiveness of artificial intelligence (AI) and machine learning techniques for VES inversion (Chaudhuri et al. 2024; Biswas 2019). While such approaches were not employed in this study, the conventional inversion method used here provided satisfactory results, with the incorporation of borehole data reducing the non-uniqueness of the inverse problem.

3.3 Self-Potential (SP) Survey Design and Data Acquisition

SP surveys were conducted along 100-metre traverses at each of the six locations, coinciding with the VES stations to enable direct correlation. The surveys employed non-polarising Cu-$CuSO_4$ electrodes (Chandra 2016; Revil et al. 2013), which consist of a copper rod immersed in a saturated copper sulphate solution contained within a porous pot. This electrode configuration minimizes electrode polarisation and drift, ensuring stable and repeatable potential measurements (Corwin and Hoover 1979).

A fixed base electrode was established at a reference point with stable potential, while a roving electrode was moved at 5-metre intervals along the traverse to measure natural potential differences relative to the base (Fig. 4). The potential difference was measured using a high-impedance voltmeter to minimize current draw and electrode polarisation. Measurements were recorded only after the potential reading stabilized (typically 30-60 seconds after electrode placement). The entire traverse was repeated in reverse direction to check for measurement consistency and to identify any drift in the base electrode potential.

SP anomalies were interpreted as indicative of groundwater flow zones (positive anomalies) or clay-rich, low-permeability zones (negative anomalies) (Corwin and Hoover 1979; Revil et al. 2003). The SP data were plotted as semi-log graphs of SP (mV) versus AB/2 (m), corresponding to the VES electrode spacing to facilitate direct depth correlation. The magnitude of the SP anomaly was determined by the difference between the maximum positive peak and the background potential, following the approach of Soupios et al. (2007). For each station, the maximum positive SP anomaly was recorded as an indicator of groundwater flow intensity.

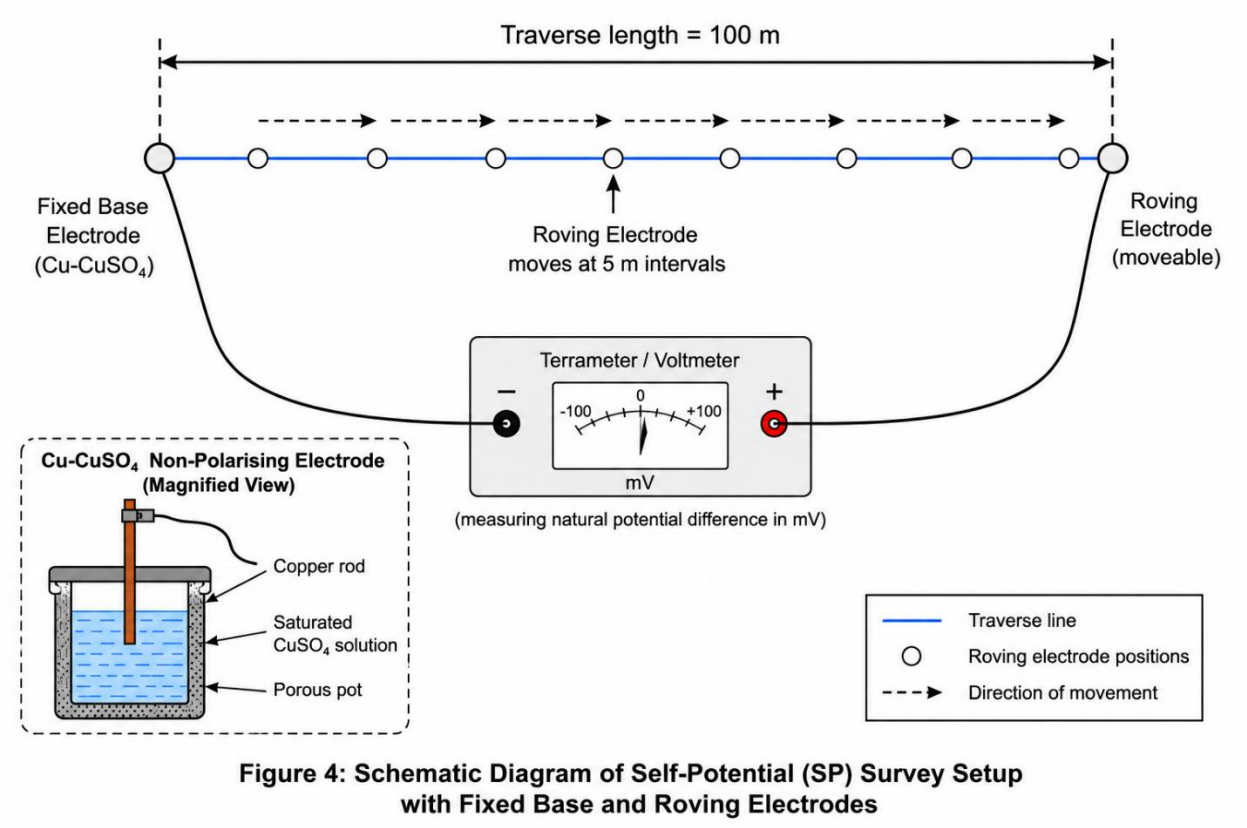


Figure 4: Schematic Diagram of Self-Potential (SP) Survey Setup with Fixed Base and Roving Electrodes

3.4 Aquifer Yield Assessment

Constant-rate pumping tests were conducted at the six boreholes located at the VES/SP stations, following the standard procedures outlined in ASTM D4050-20 (2020) and Kruseman and de Ridder (1990). Each test consisted of 120 minutes of pumping followed by 60 minutes of recovery monitoring. Submersible pumps were installed at depths of 5-10 m below the static water level, with discharge rates maintained between 36.7 and 45.2 L/min using flow control valves and flow meters (± 0.5 L/min accuracy). The pumping rate was chosen based on the maximum sustainable yield of each borehole determined from prior step-drawdown tests.

Drawdown was monitored at regular intervals (1, 2, 3, 4, 5, 6, 7, 8, 9, 10, 12, 14, 16, 18, 20, 25, 30, 40, 50, 60, 80, 100, and 120 minutes) using both pressure transducers (accuracy ± 1 cm) and manual dipmeter measurements to ensure data quality and redundancy. Water level readings were corrected for pumping rate variations where necessary. The test was terminated when drawdown stabilized or when 120 minutes elapsed.

Specific capacity was calculated as the ratio of pumping rate to drawdown (Q/s), a standard indicator of well performance and aquifer productivity (Kruseman and de Ridder 1990; Mace 2001). Specific capacity is inversely related to drawdown and provides a measure of the transmissive properties of the aquifer.

Transmissivity (T) was estimated using the Cooper-Jacob straight-line method (Cooper and Jacob 1946; Kruseman and de Ridder 1990), which applies to the pumping test data obtained under the following conditions: (1) the aquifer is confined or unconfined with delayed yield effects minimized; (2) the well fully penetrates the aquifer; and (3) the pumping period is sufficiently long for the straight-line portion of the drawdown versus log time curve to develop. The transmissivity was calculated using:

$T = (2.303Q)/(4\pi\Delta s)$

where T is transmissivity (m^2/day), Q is pumping rate (m^3/day), and Δs is the drawdown difference per log cycle of time (m), determined from the slope of the semi-log plot of drawdown versus time (Fig. 5). The coefficient of determination (R^2) for the straight-line fit was > 0.95 for all tests, indicating reliable transmissivity estimates.

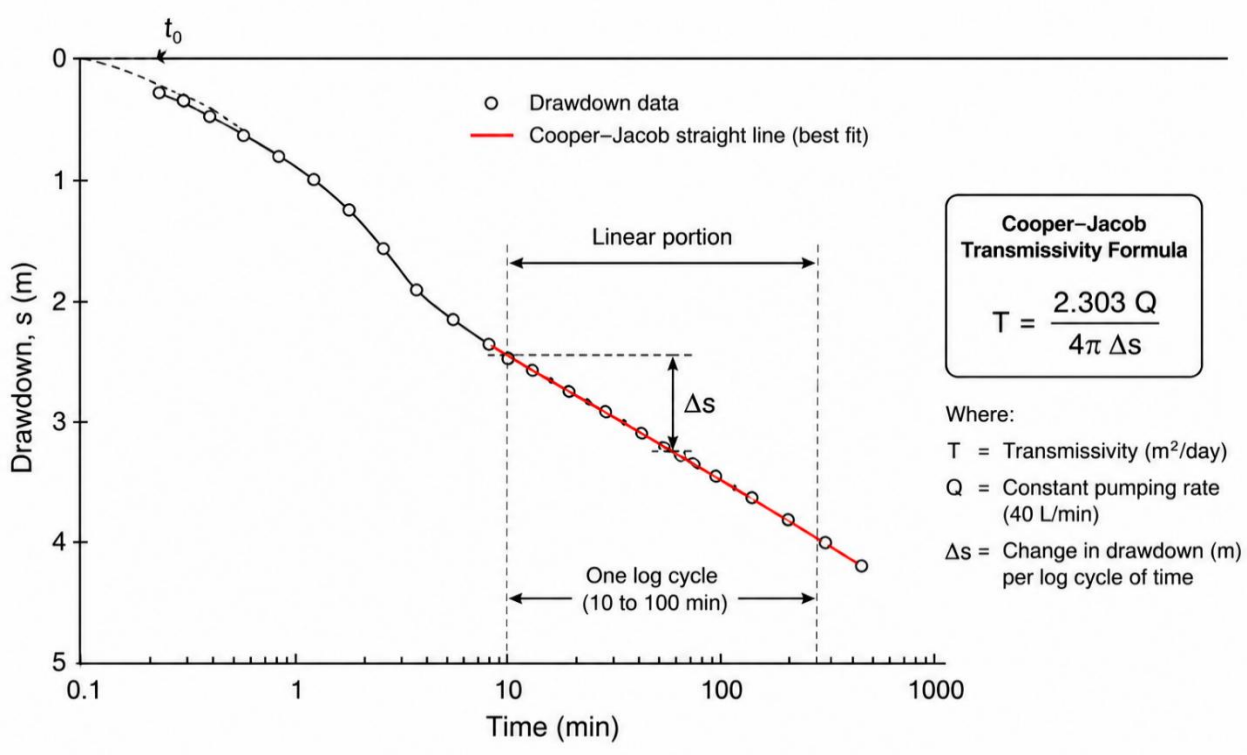


Figure 5: Semi-log Plot of Drawdown versus Time for a Representative Borehole (Cooper-Jacob Method)

3.5 Groundwater Potential Zonation

Groundwater potential was determined through the integration of geophysical and hydraulic parameters that serve as reliable indicators of aquifer productivity in crystalline basement terrains. The following parameters and criteria were employed (Table 1):

Aquifer thickness (m): Greater thickness indicates higher storage capacity, as the weathered zone provides the primary storage volume in basement aquifers (Olorunfemi and Fasuyi 1993; Adiat et al. 2009). Thicknesses > 10 m were considered favorable for groundwater development.

Aquifer resistivity (Ωm): Resistivity values between 20 and 300 Ωm indicate saturated, permeable weathered basement material (Olorunfemi and Ojo 2003; Adiat et al. 2009). Lower resistivity (< 20 Ωm) may indicate clay-rich materials with low permeability, while higher resistivity (> 300 Ωm) suggests unsaturated or low-porosity materials.

SP anomaly (mV): Positive SP anomalies ≥ +100 mV indicate active groundwater flow through porous media or fractures (Revil et al. 2003; Soupios et al. 2007). The magnitude of the positive anomaly is proportional to the intensity of groundwater movement.

Basement type: Fractured basement (resistivity < 1000 Ωm) enhances permeability and borehole yield, while fresh basement (resistivity > 1000 Ωm) acts as an impermeable barrier. The ratio of weathered to fractured basement influences overall aquifer productivity (Olorunfemi and Ojo 2003).

A composite groundwater potential rating was assigned to each location based on the integration of these parameters, with classifications of Very High, High, Moderate, and Low potential.

Table 1: Aquifer Potential Zoning

Parameter	**Indicator of High Potential**	**Reference**
Aquifer thickness (m)	Greater thickness = higher storage capacity	(Olorunfemi & Fasuyi, 1993; Adiat et al.,2009).
Aquifer resistivity (Ωm)	20-300 Ωm = saturated, permeable zone	Olorunfemi & Ojo (2003); Adiat et al. (2009)
SP anomaly (mV)	≥ +100 mV = active groundwater flow	Revil et al. (2003); Soupios et al. (2007)

3.6 Data Integration and Spatial Analysis

Geophysical and hydraulic data were integrated within a Geographic Information System (GIS) framework using ArcGIS 10.8 (ESRI 2019). All data were georeferenced to the WGS 84 coordinate system using GPS measurements collected at each VES/SP station. Attribute tables were created for each dataset, containing station coordinates, VES parameters (resistivity and thickness of each layer), SP anomaly values, and pumping test results.

Inverse Distance Weighting (IDW) interpolation was employed to generate continuous surface maps of aquifer thickness and groundwater potential (Watson and Philip 1985). IDW is a deterministic interpolation method that assigns weights to sampled points based on their distance from the prediction location, with nearer points receiving greater weights. A power parameter of 2 was selected to balance local detail with smoothness, and a fixed search radius of 500 m was used to ensure adequate point coverage.

Correlation analysis between geophysical parameters (aquifer resistivity, maximum SP anomaly) and hydraulic parameters (specific capacity, transmissivity) was performed using Pearson correlation coefficients at 95% confidence intervals ($p < 0.05$) using SPSS v.26 (IBM Corp. 2019).

The correlation matrix was constructed to identify significant relationships among variables, providing insights into the factors controlling aquifer productivity.

A methodological flowchart (Fig. 6) summarizes the sequence of data acquisition, processing, integration, and interpretation.

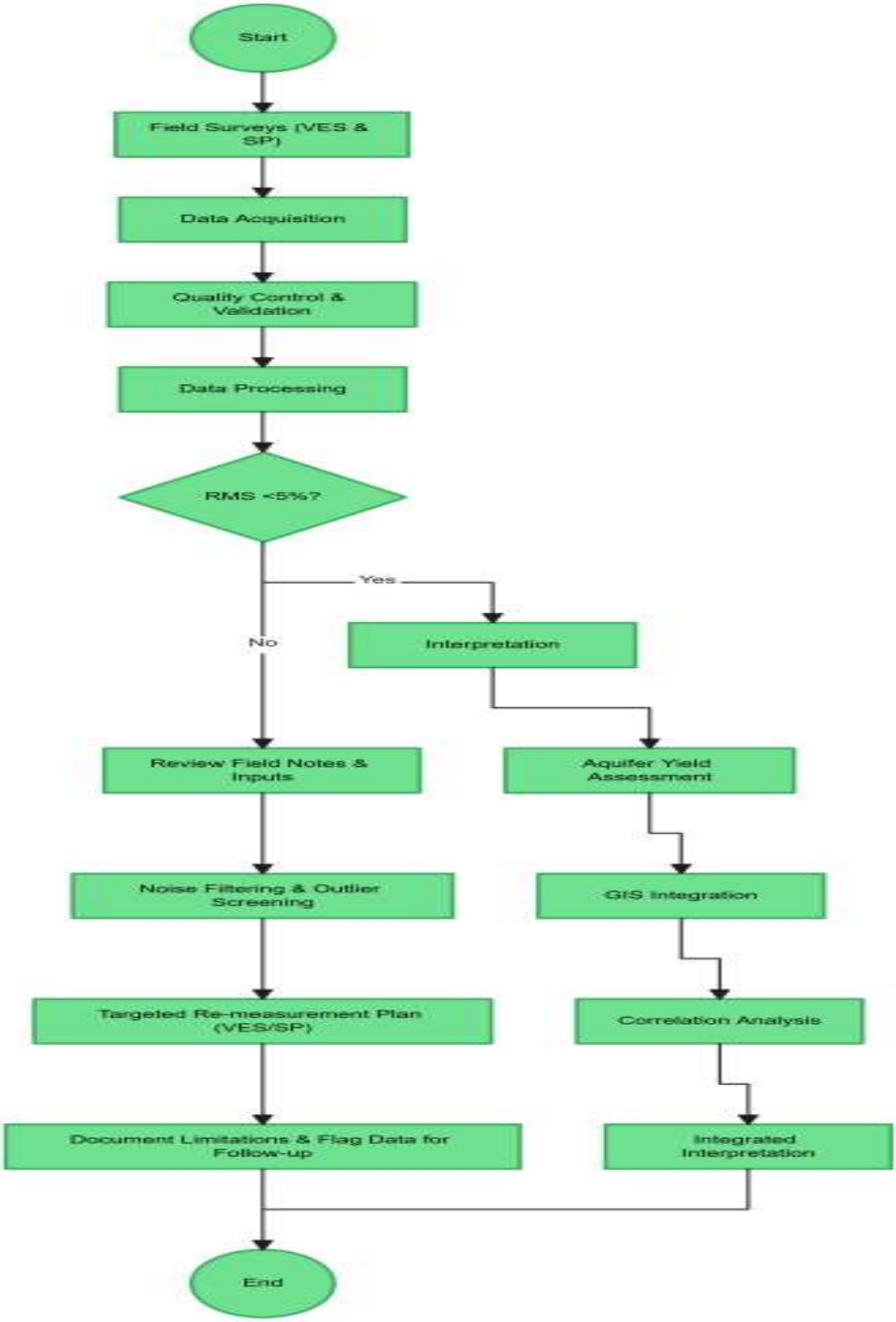


Figure 6: Methodological Flowchart for Geophysical Data Acquisition, Processing, and Integration

4. RESULTS

4.1 Vertical Electrical Sounding (VES)

Six VES points were quantitatively interpreted using the iterative optimization algorithm implemented in RESIST software (Vander Velpen 1988). The field curves were re-plotted on bi-logarithmic (log-log) scales (Figs. 7-12), which is the standard presentation for geoelectrical sounding data. The inversion process minimized the RMS error between measured and calculated apparent resistivity values; all final models achieved RMS errors below 5% (range: 1.2-4.7%), indicating excellent model-data fit (Table 2).

VES 1 (Multipurpose Complex) The sounding curve is classified as KH-type ($\rho_1 < \rho_2 > \rho_3 < \rho_4$), indicating two resistivity maxima separated by a minimum. The four-layer model comprises: (1) topsoil (174 Ωm, 0.9 m) - sandy clay with moderate resistivity; (2) lateritic clay (265 Ωm, 4.2 m) - relatively resistive due to iron oxide cementation; (3) weathered basement (121 Ωm, 6.7 m) - saturated weathered amphibolite schist; and (4) fractured/fresh basement (205 Ωm) - indicating some fracturing beneath the weathered zone. The KH-type pattern, with a conductive middle layer (Layer 3) sandwiched between more resistive materials, is characteristic of a weathered profile over fractured basement in basement terrains (Orellana and Mooney 1966).

VES 2 (Multidisciplinary Research Building) The curve is classified as QH-type ($\rho_1 > \rho_2 > \rho_3 < \rho_4$), showing a descending sequence with a sharp resistivity rise in the deepest layer. The thick, low-resistivity Layer 3 (109 Ωm, 21.9 m) represents a water-saturated weathered basement with a near-surface water table (indicated by the low resistivity). The underlying Layer 4 (233 Ωm) is interpreted as fractured/fresh basement. The QH-type curve reflects a pronounced resistivity minimum associated with the saturated zone, which is the most favorable VES curve type for groundwater occurrence in basement terrains (Olorunfemi and Fasuyi 1993; Adiat et al. 2009). The considerable thickness of the weathered zone (21.9 m) and its low resistivity suggest high groundwater storage capacity.

VES 3 (Anatomy Complex) The curve is K-type (ascending: $\rho_1 < \rho_2 < \rho_3$), indicating a progressive increase in resistivity with depth. The three-layer model consists of: (1) topsoil (390 Ωm, 1.6 m) - sandy clay with high resistivity; (2) weathered basement (171 Ωm, 11.6 m) - moderately saturated weathered material; and (3) extremely resistive fresh basement (10,271 Ωm) - indicating competent, unweathered bedrock. The dramatic rise in resistivity at larger AB/2 values indicates fresh basement with negligible permeability. The K-type curve in crystalline terrains typically indicates a lack of significant fracture development, limiting groundwater potential.

VES 4 (Engineering Building) The curve is classified as QH-type ($\rho_1 > \rho_2 > \rho_3 < \rho_4$), similar to VES 2 but with a much more pronounced resistivity minimum. The four-layer model shows: (1) thin topsoil (515 Ωm, 0.6 m); (2) lateritic clay (117 Ωm, 11.7 m); (3) highly conductive weathered basement (30 Ωm, 15.7 m) - representing very saturated weathered material; and (4) fractured basement (418 Ωm). The curve reaches a minimum apparent resistivity around AB/2 = 40 m, typical of a thick, conductive aquifer. The extremely low resistivity of Layer 3 (30 Ωm) is

diagnostic of a highly saturated formation with significant water content. The underlying fractured basement (418 Ωm) indicates a zone of enhanced permeability, providing the ideal combination for high groundwater productivity.

VES 5 (Behind ATM Stand) The curve is QH-type ($\rho_1 > \rho_2 > \rho_3 < \rho_4$) with a less pronounced minimum than VES 4. The four layers are: (1) topsoil (699 Ωm, 1.0 m); (2) lateritic clay (265 Ωm, 11.0 m); (3) weathered basement (145 Ωm, 23.3 m) - thick but moderately resistive; and (4) fresh basement (560 Ωm). While this location has the thickest weathered zone (23.3 m), the higher resistivity (145 Ωm) suggests lower saturation or finer-grained material with reduced permeability compared to VES 2 and VES 4. The fresh basement with no fracture signature limits permeability despite the substantial storage capacity.

VES 6 (Staff Office) The curve is K-type (ascending: $\rho_1 < \rho_2 < \rho_3$), similar to VES 3. The three-layer model comprises: (1) topsoil (197 Ωm, 0.9 m); (2) a thin laterite/compacted sand layer (113 Ωm, 3.8 m); and (3) fresh basement (245 Ωm). The thin conductive layer and the rapid rise to basement resistivities indicate very limited groundwater potential. The K-type curve with a thin weathered layer suggests an area where weathering has been minimal, and the fresh basement is at shallow depth.

Table 2: Geoelectric Parameters and Inferred Lithology from VES Interpretation								
VES POINTS	**Location Description**	**Curve Type**	**Layer**	**Resistivity (Ωm)**	**Thickness (m)**	**Depth (m)**	**Inferred Lithology**	**R.M.S Error (%)**
VES 1	Multipurpose Complex	KH	1	174	0.9	0.9	Top Soil (Sandy clay)	3.2
			2	265	4.2	5.1	Lateritic Clay layer	
			3	121	6.7	11.8	Weathered Basement	
			4	205	-	-	Fractured/Fresh Basement	
VES 2	Multidisciplinary Research Building	QH	1	318	0.6	0.6	Thin Top Soil (Sandy clay)	2.8
			2	236	5.0	5.6	Lateritic Clay layer	
			3	109	21.9	27.5	Water-Saturated Weathered basement material (Near surface water table)	
			4	233	-	-	Fractured/Fresh Basement	
VES 3	Anatomy Complex	K	1	390	1.6	1.6	Top Soil	1.6
			2	171	11.6	13.3	Weathered Basement	
			3	10,271	-	-	Highly Fresh Basement Rock	
VES 4	Engineering Building	QH	1	515	0.6	0.6	Thin Top Soil	3.4
			2	117	11.7	12.2	Lateritic Clay Materials	
			3	30	15.7	27.9	Weathered Basement layer (very saturated weathered formation)	
			4	418	-	-	Fresh/fractured Basement Rock	
VES 5	Behind the ATM Stand/SET Building	QH	1	699.0	1.0	1.0	Top Soil	4.7
			2	265	11.0	12.1	Lateritic Clay	
			3	145	23.3	35.4	Weathered Basement layer	

			4	560	-	-	Fresh Basement Rock	
VES 6	Staff Office	K	1	197	0.9	0.9	Top Soil	1.8
			2	113	3.8	4.7	Laterite/Compacted Sand	
			3	245	-	-	Fresh Basement	

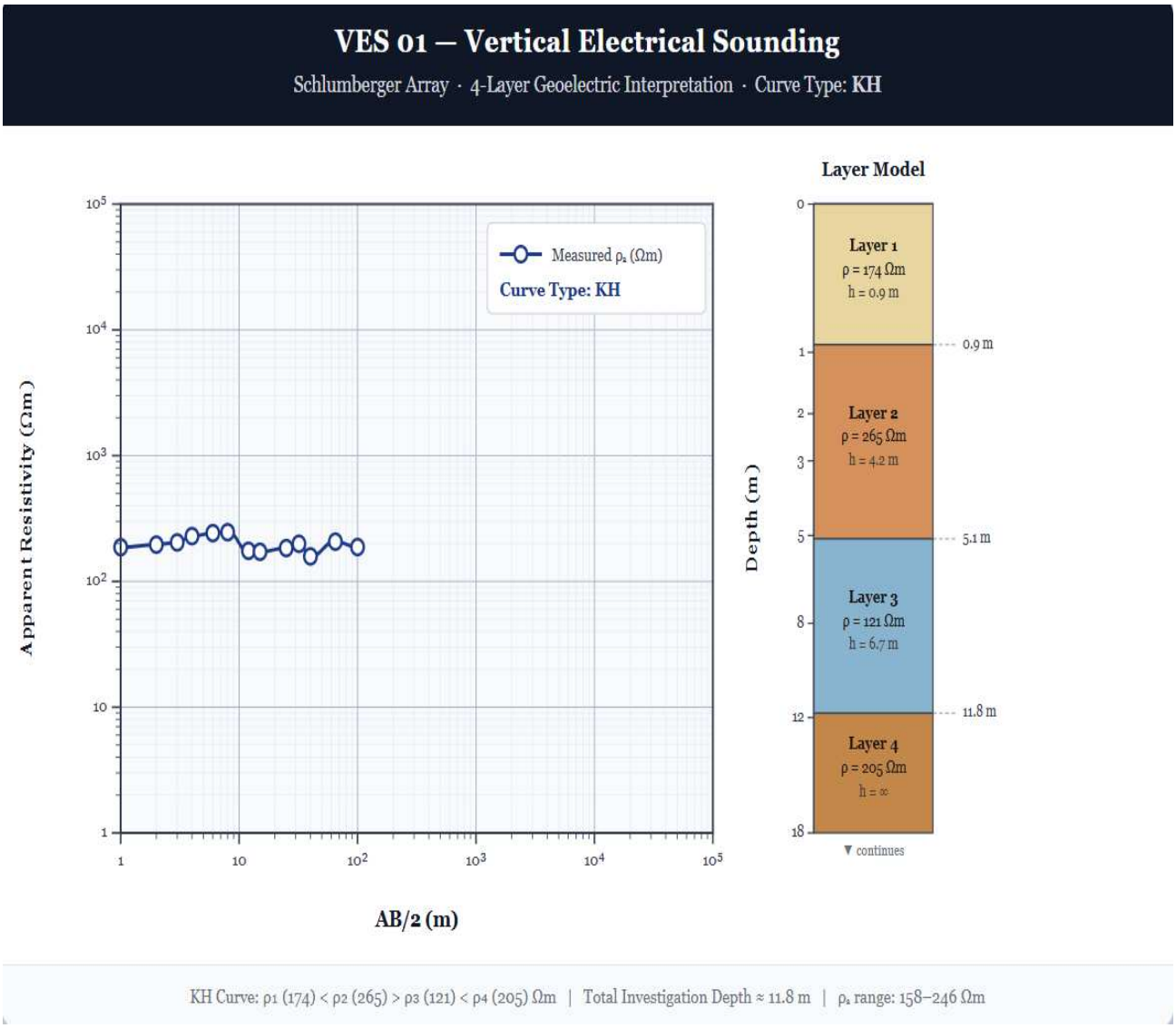


Figure 7: VES 1 Inversion Model Showing Geoelectric Layers at Multipurpose Complex.

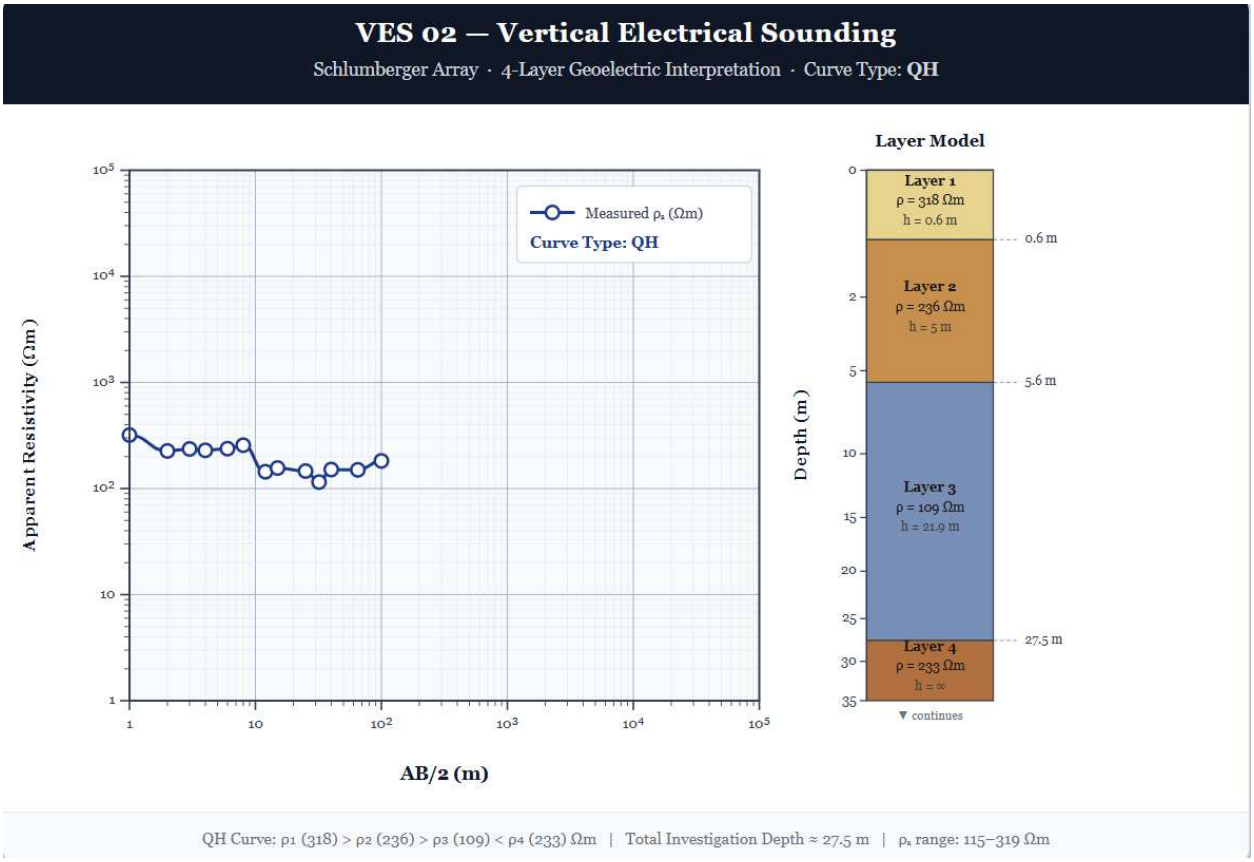


Figure 8: VES 02 Inversion Model Showing Geoelectric Layers at Multidisciplinary Research Building.

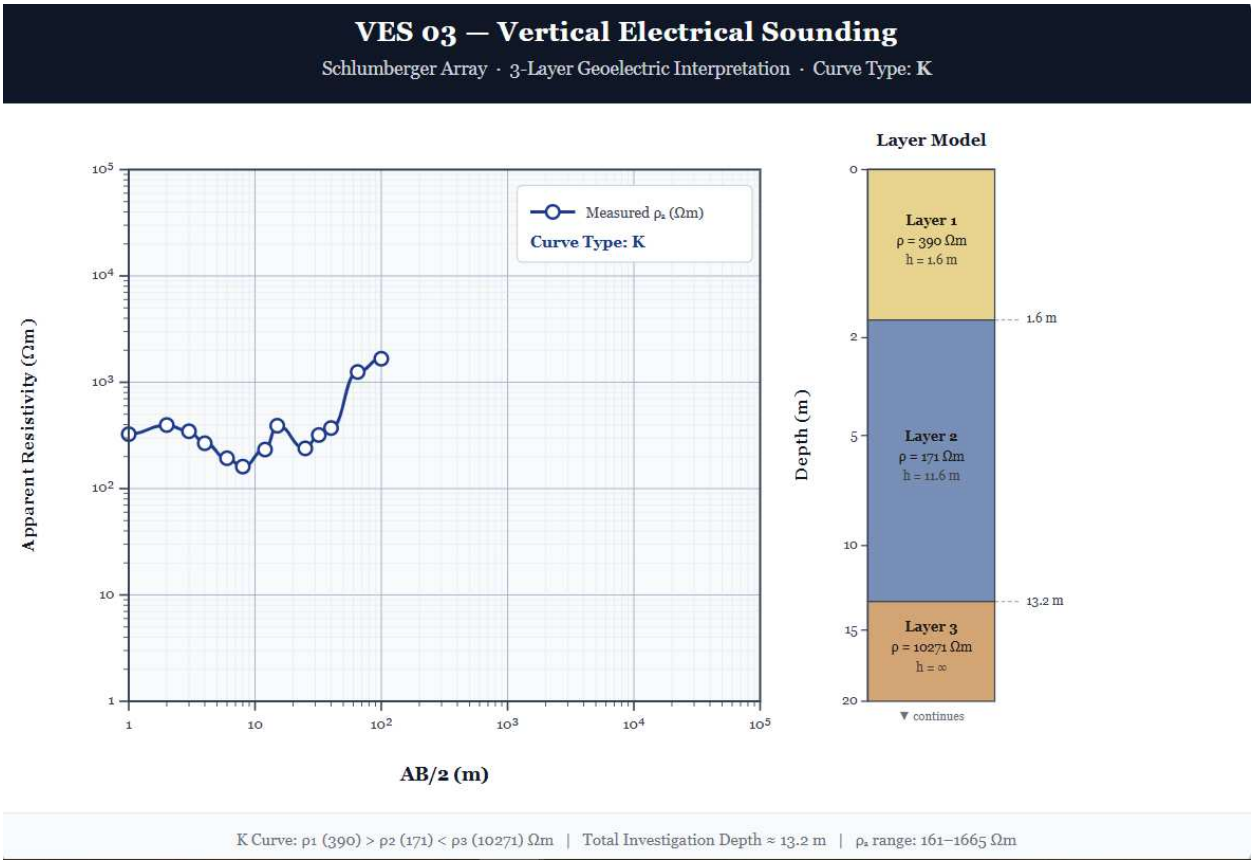


Figure 9: VES 03 Inversion Model Showing Geoelectric Layers at Anatomy Complex.

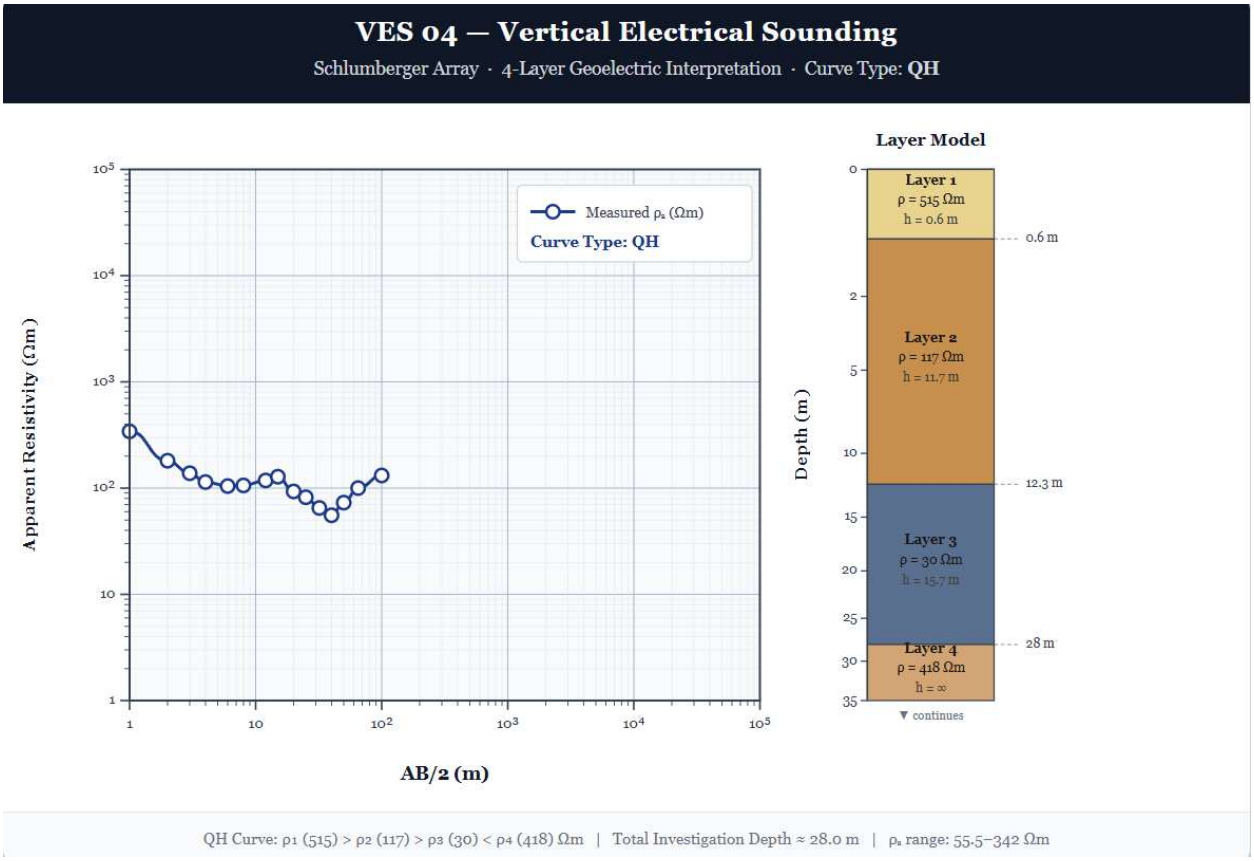


Figure 10: VES 04 Inversion Model Showing Geoelectric Layers at the Engineering Building.

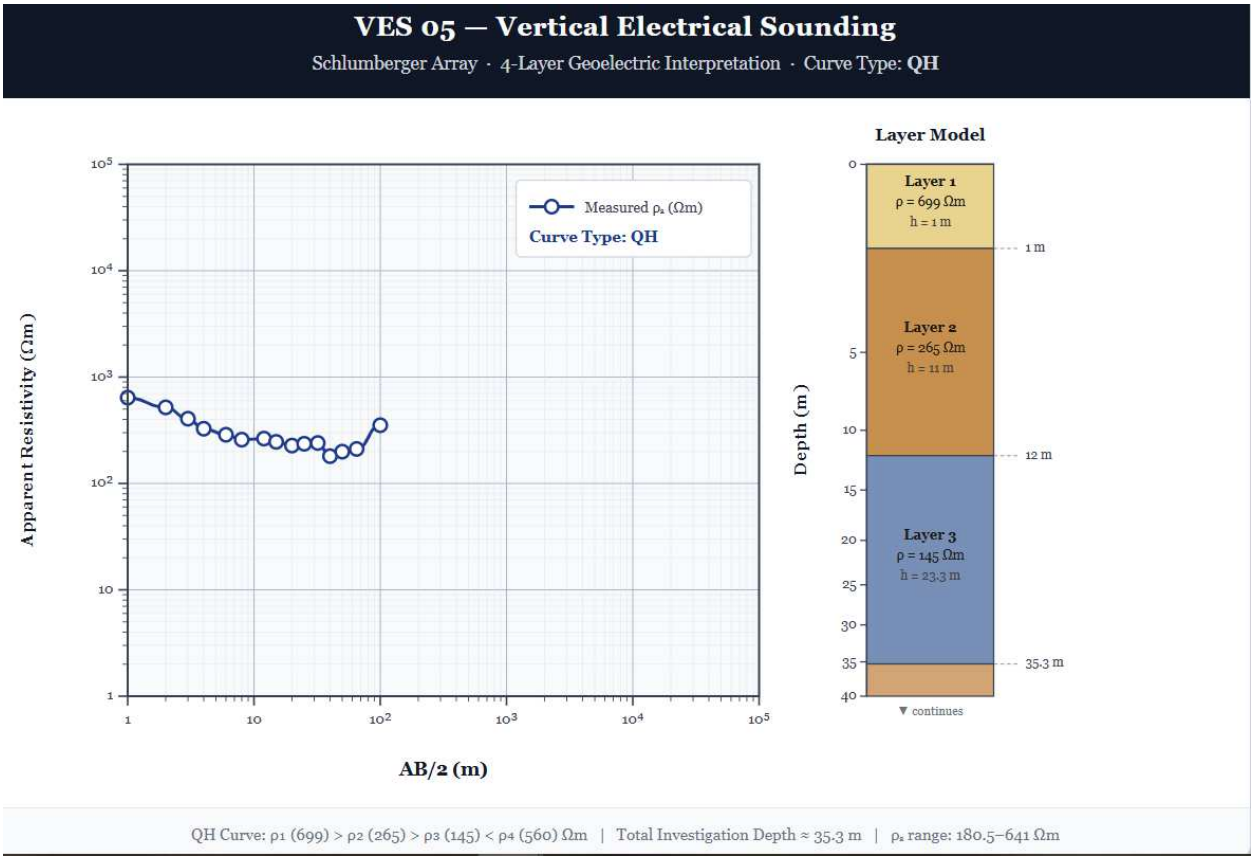


Figure 11: VES 05 Inversion Model Showing Geoelectric Layers at SET Building.

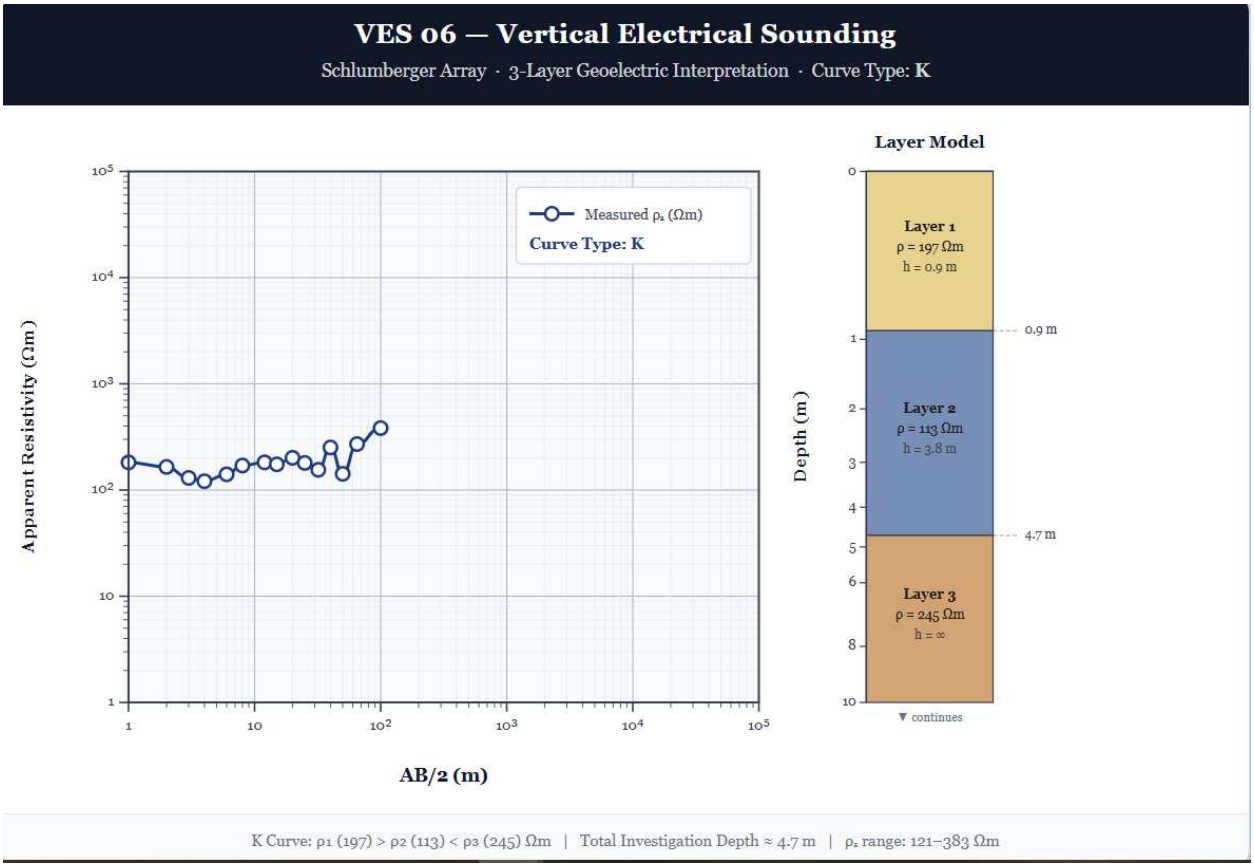


Figure 12: VES 06 Inversion Model Showing Geoelectric Layers at Staff Office Building.

4.2 Aquifer Characterization by Location

The following assessment integrates the VES curve types (Table 2), the interpreted layer parameters, and the corresponding groundwater potential.

VES 4 (Engineering Building) - QH-type curve ($\rho_1 > \rho_2 > \rho_3 < \rho_4$). This location exhibits the most favourable aquifer geometry. The very low resistivity of Layer 3 (30 Ωm, thickness 15.7 m) is diagnostic of a highly saturated weathered basement formation. The sharp resistivity minimum on the sounding curve (around AB/2 = 40 m) corresponds to this thick conductive layer. It is underlain by a more resistive fractured basement (418 Ωm). This configuration provides both substantial storage (thick saturated zone) and enhanced permeability (underlying fractures). Groundwater potential: **very high.**

VES 2 (Multidisciplinary Research Building) - QH-type curve ($\rho_1 > \rho_2 > \rho_3 < \rho_4$). The thick, low-resistivity Layer 3 (109 Ωm, 21.9 m) represents a water-saturated weathered basement with a near-surface water table. The QH-type character reflects a pronounced resistivity minimum associated with this saturated zone. The underlying fractured/fresh basement (233 Ωm) enhances vertical permeability. Groundwater potential: **high.**

VES 5 (Behind ATM Stand) - QH-type curve ($\rho_1 > \rho_2 > \rho_3 < \rho_4$). Although this location has the thickest weathered zone (23.3 m), its resistivity (145 Ωm) is higher than that of VES 2 and VES 4, indicating lower saturation or finer-grained material. The QH-type curve shows a less pronounced minimum, and the underlying basement is fresh rock (560 Ωm) with no distinct fracture signature. Groundwater potential: **moderate.**

VES 3 (Anatomy Complex) - K-type curve (ascending: $\rho_1 < \rho_2 < \rho_3$). The weathered basement layer is of moderate thickness (11.6 m, 171 Ωm). The K-type curve rises steeply at larger AB/2 values, culminating in extremely resistive fresh basement (10,271 Ωm). The absence of a low-resistivity or fractured layer limits permeability, despite reasonable storage capacity. Groundwater potential: **moderate.**

VES 1 (Multipurpose Complex) - KH-type curve ($\rho_1 < \rho_2 > \rho_3 < \rho_4$). This four-layer model includes a thin weathered basement layer (6.7 m, 121 Ωm) underlain by fractured/fresh basement (205 Ωm). The KH-type pattern is present, but the conductive layer is very thin. The limited thickness of the saturated zone restricts sustainable yield. Groundwater potential: **low to moderate.**

VES 6 (Staff Office) - K-type curve (ascending: $\rho_1 < \rho_2 < \rho_3$). Only three layers are present: topsoil, a thin laterite/compacted sand layer (113 Ωm, 3.8 m), and fresh basement (245 Ωm). The rapidly ascending K-type curve reflects the absence of a thick weathered aquifer. The thin conductive layer offers very little storage, and the fresh basement provides no permeability. Groundwater potential: **low.**

4.3 Self-Potential (SP) Survey Results

The SP measurements were acquired using the same Schlumberger array as the VES, with readings taken at each AB/2 spacing. Therefore, the SP data are plotted as semi-log graphs of SP (mV) versus AB/2 (m) (Figs. 13-18). Positive SP anomalies indicate zones of active groundwater flow, while negative anomalies suggest limited movement or clay-rich, low-permeability materials (Corwin & Hoover, 1979; Revil et al., 2003). The depth of investigation is approximately 0.5-1.0 times the AB/2 spacing (Telford et al., 1990). The main features of each SP sounding are summarised in Table 3.

Table 3: Self-Potential Data and Groundwater Potential Rating

SP Station	Location Description	SP Anomaly Characteristics	Peak/Nadir Values (mV)	AB/2 (m) / Inferred Depth	Interpretation of Groundwater Flow	Groundwater Potential
SP 1	Multipurpose Complex	Strong negative dip followed by a sharp positive rise	-110 to +100	Negative at 6-8 m (≈4-6 m depth); positive at 40-65 m (≈25-45 m depth)	Transition from clay (negative) to saturated weathered basement (positive); slow movement	Moderate

SP 2	Multidisciplinary Research Building	Consistent gradual increase, no sharp fluctuations	Up to +200	Broad positive from 15-40 m (≈10-30 m depth)	Well-saturated porous formation with lateral flow; uniform movement	Good
SP 3	Anatomy Complex	Moderate increase, then stabilization	Up to +70	Positive at 32-40 m (≈20-30 m depth); negative at 15 m and 100 m	Limited groundwater flow; semi-saturated layer; no fractured basement	Moderate
SP 4	Engineering Building	Sharp prominent peak (highest anomaly)	Up to +700	Extreme +705 mV at 32 m (≈21 m depth)	Pressurized/confined aquifer; strong water movement within a thick saturated weathered zone	Very High
SP 5	Behind the ATM Stand/SET Building	Low, relatively flat, entirely negative	~ -110 (range -13.8 to -103)	Negative across all AB/2 (2-100 m)	Poor water movement, limited saturation; clayey/compacted layers restrict flow	Low
SP 6	Staff Office Building	Sharp drop then sharp rise (bipolar)	-180 to +170	Negative at 1-2 m (≈1-2 m); positive at 6 m (≈4-5 m) and 100 m (≈60 m)	Water moving from a dry/resistive zone into a conductive saturated formation; electrochemical boundary	Moderate (bipolar, but thin aquifer limits yield)

Note: Inferred depth ≈ AB/2 for Schlumberger array (Telford et al., 1990).

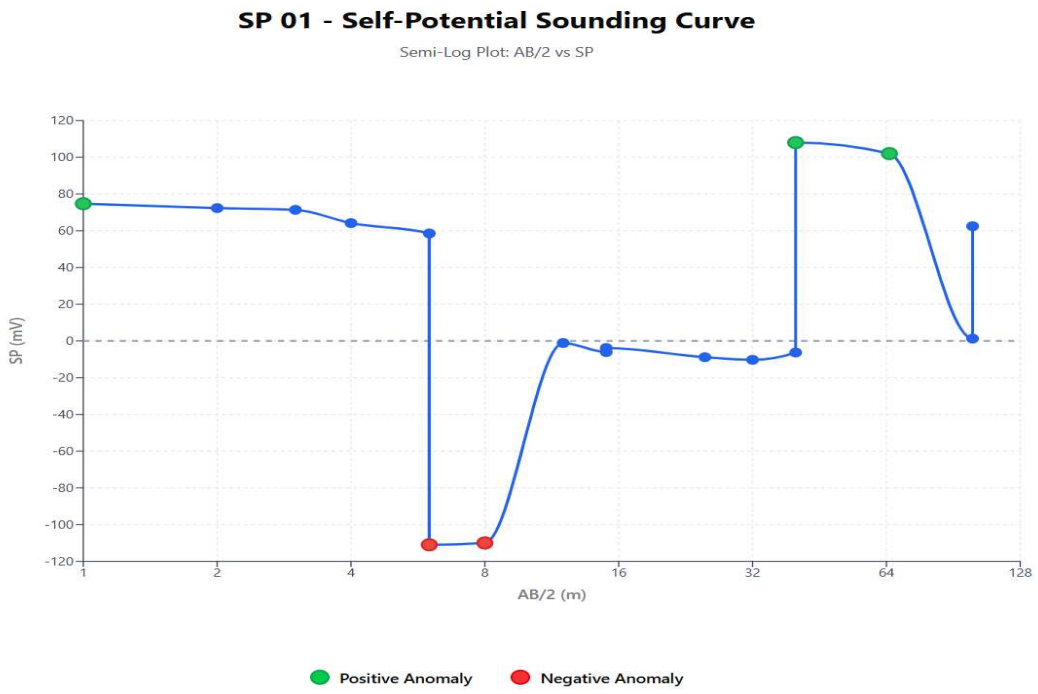


Figure 13: SP Profile at Multipurpose Complex (SP 1)

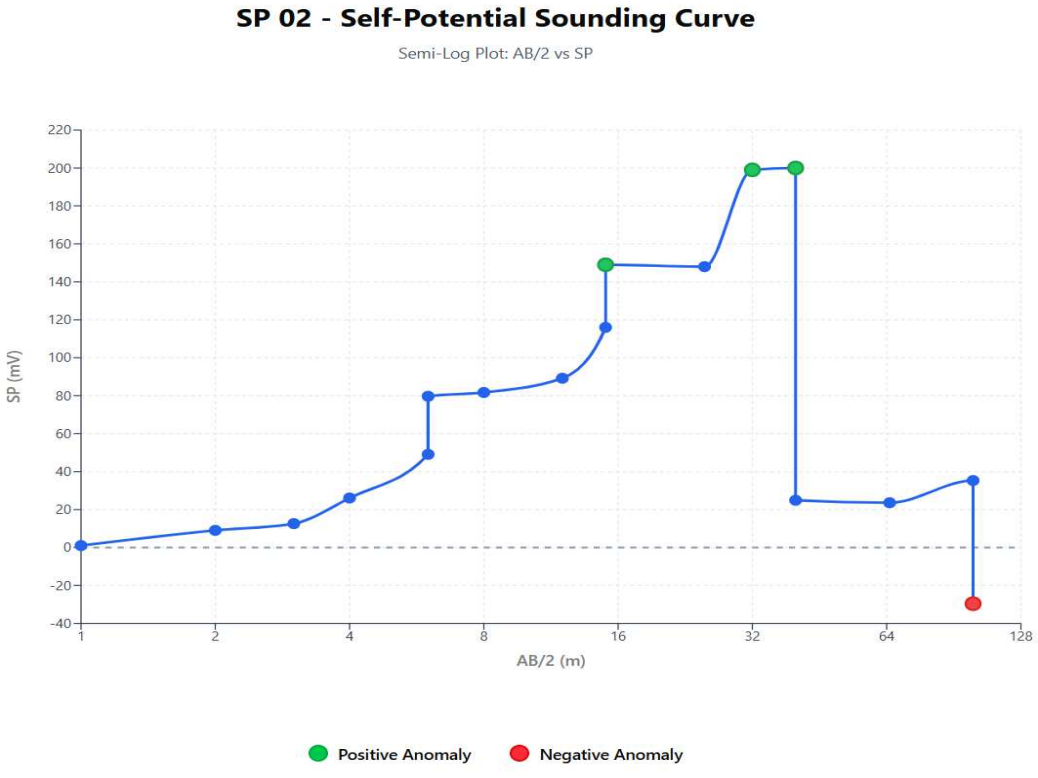


Figure 14: SP Profile at Multidisciplinary Research Building (SP 2)

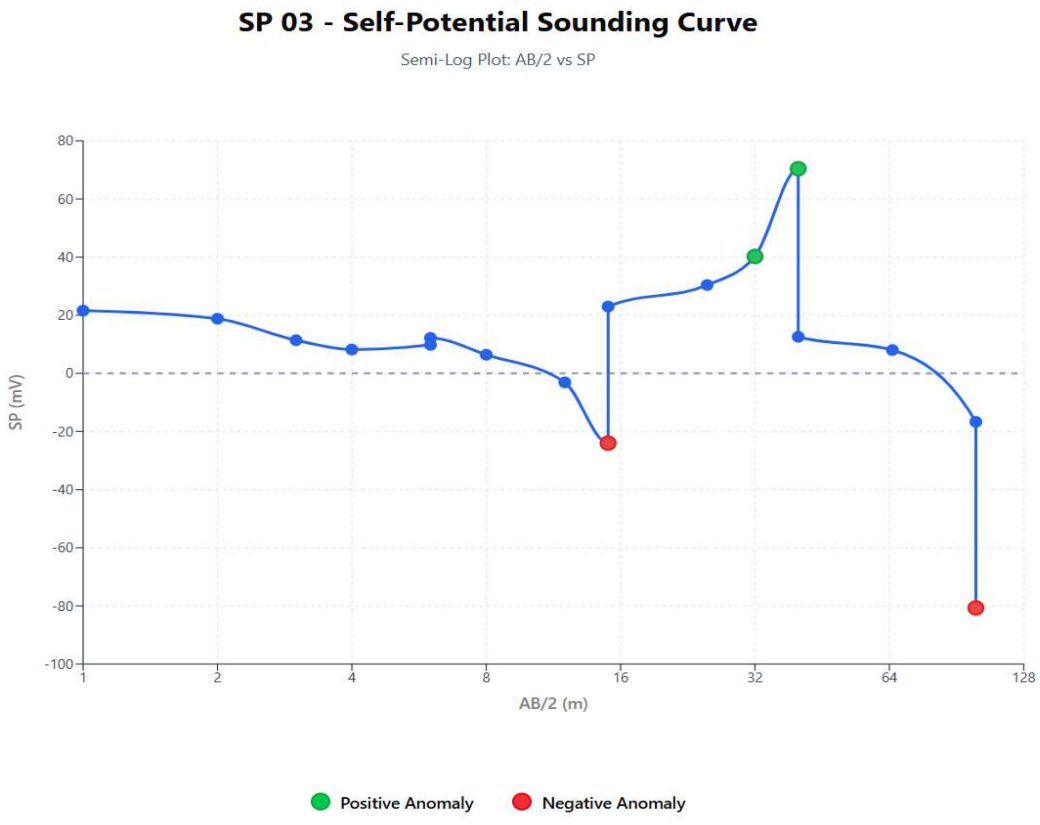


Figure 15: SP Profile Opposite Anatomy Complex (SP 3)

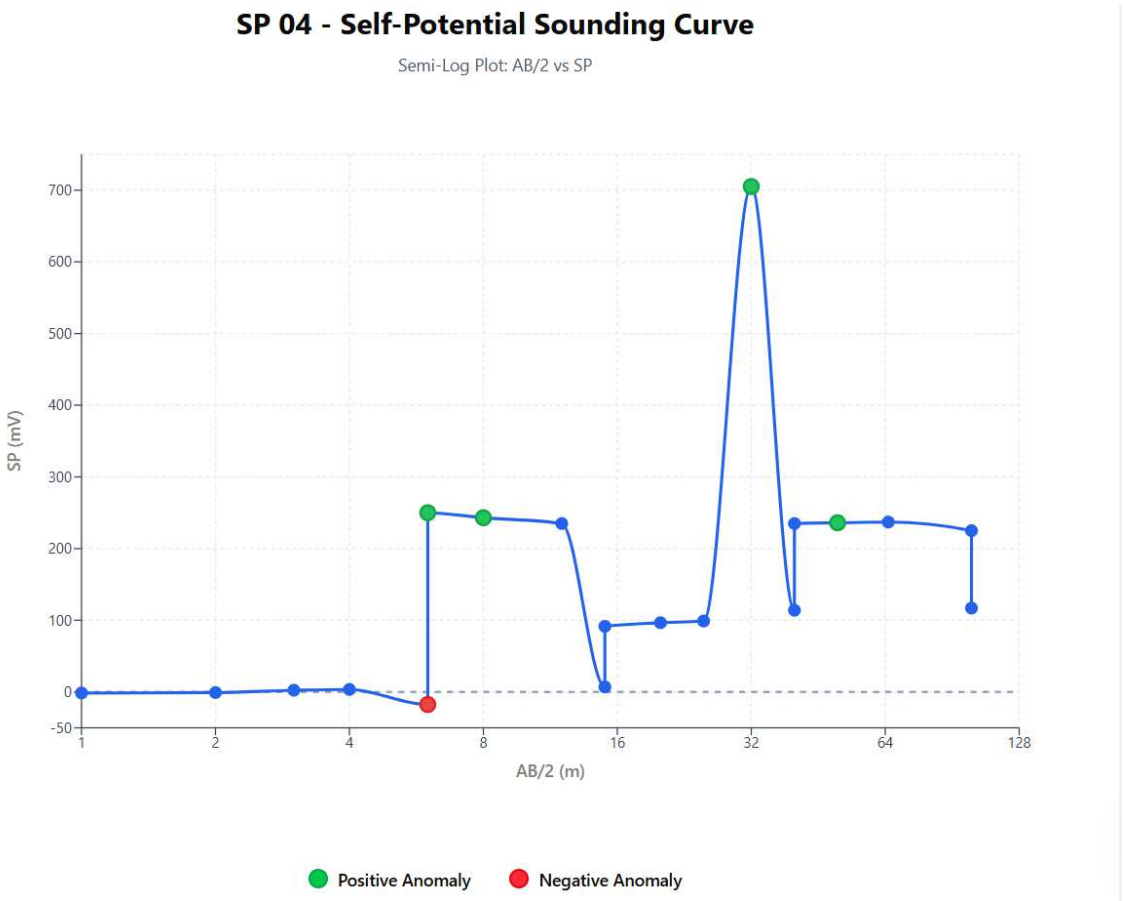


Figure 16: SP Profile in Front of Engineering Building (SP 4)

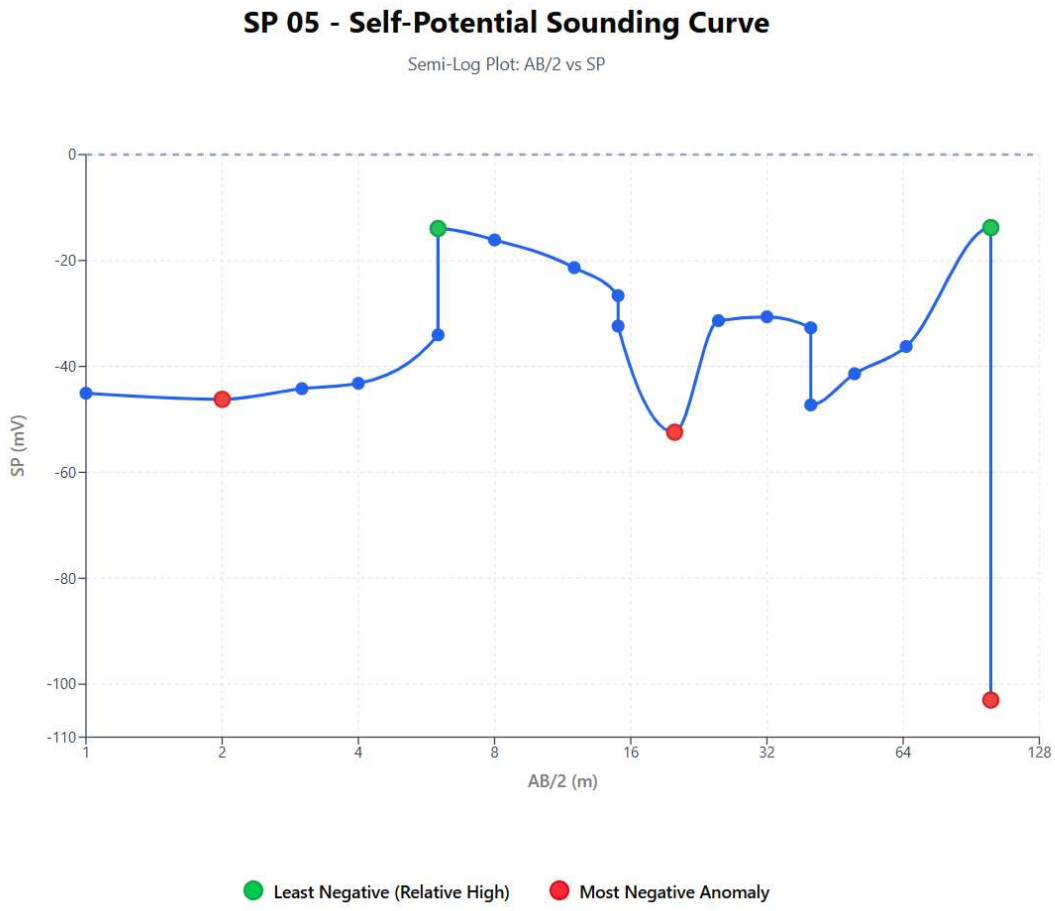


Figure 17: SP Profile SET Building (SP 5)

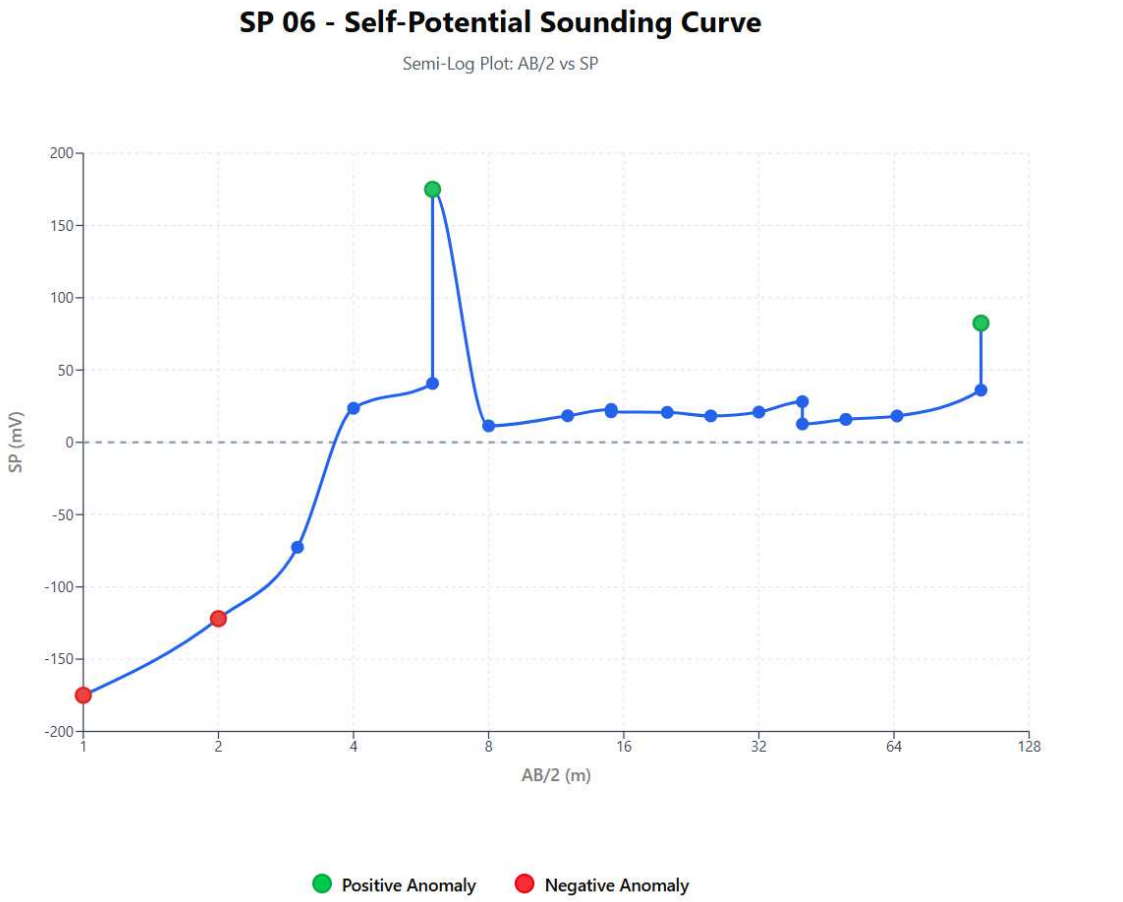


Figure 18: SP Profile Staff Office Building (SP 6)

SP 1 (Multipurpose Complex - Fig. 13) The curve shows a strong negative anomaly at AB/2 = 6-8 m (−111 mV to −110 mV), followed by a sharp rise to positive values at AB/2 = 40 m (+108 mV) and 65 m (+102 mV). The negative anomaly coincides with the lateritic clay layer (resistivity 265 Ωm, depth ≈ 5 m). The positive peaks correspond to the weathered basement (resistivity 121 Ωm, depths ≈ 20-35 m). The transition from negative to positive indicates a change from clay-dominated to water-saturated permeable material. Groundwater potential: **moderate.**

SP 2 (Multidisciplinary Research Building - Fig. 14) This profile is predominantly positive, with a strong ascending trend. Positive anomalies are recorded at AB/2 = 15 m (+149 mV), 32 m (+199 mV), and 40 m (+200 mV). A weak negative anomaly occurs at AB/2 = 100 m (−29.6 mV). The broad, consistent positive response (up to +200 mV) between AB/2 = 15-40 m indicates a thick, well-saturated, porous formation with lateral groundwater flow - corresponding to the water-saturated weathered basement (109 Ωm, 21.9 m thick, top at ≈5.6 m). Groundwater potential: **good.**

SP 3 (Anatomy Complex - Fig. 15) The SP profile is variable, with both positive and negative anomalies. Positive peaks occur at AB/2 = 32 m (+40.2 mV) and 40 m (+70.4 mV). Negative anomalies are seen at AB/2 = 15 m (−24.0 mV) and 100 m (−80.7 mV). The positive anomalies are modest, suggesting limited groundwater flow within the weathered basement (171 Ωm, 11.6 m thick). The lack of a strong, sustained positive response is consistent with the absence of a fractured basement. Groundwater potential: **moderate.**

SP 4 (Engineering Building - Fig. 16) This profile exhibits remarkably high positive SP anomalies. The most significant features are: AB/2 = 6 m (+250 mV), 8 m (+243 mV), 32 m (+705 mV - extreme anomaly), and 50 m (+236 mV). A small negative anomaly occurs at AB/2 = 6 m (−17.5 mV). The extreme positive anomaly at AB/2 = 32 m (+705 mV) corresponds to a depth of approximately 21 m, which coincides exactly with the very low-resistivity saturated weathered basement layer (30 Ωm, 15.7 m thick, top at 12.2 m). This indicates a pressurized or confined aquifer with exceptionally strong water movement. Groundwater potential: **very high.**

SP 5 (Behind ATM Stand - Fig. 17) This profile is unique in that it shows entirely negative SP values across the entire AB/2 range (−13.8 to −103 mV). The least negative (relative highs) occur at AB/2 = 6 m (−14.0 mV) and 100 m (−13.8 mV); the most negative are at AB/2 = 2 m (−46.2 mV), 20 m (−52.4 mV), and 100 m (−103 mV - extreme). The consistently negative response indicates poor water movement and limited saturation, despite the thick weathered zone (23.3 m, 145 Ωm). The negative SP is attributed to clay-rich, fine-grained material that restricts permeability. Groundwater potential: **low.**

SP 6 (Staff Office - Fig. 18) This profile displays a dramatic bipolar SP signature: strong negative anomalies at shallow AB/2 = 1 m (−175 mV) and 2 m (−122 mV), followed by a sharp transition to strong positive anomalies at AB/2 = 6 m (+175 mV) and 100 m (+82.5 mV). The symmetry between extreme negative and positive values (−175 mV vs. +175 mV) suggests a distinct electrochemical boundary or redox front in the shallow subsurface, with the transition occurring between AB/2 = 2-6 m (≈3-4 m depth). This pattern is characteristic of a water table, oxidation-reduction zone, or lithological contact. However, the thin weathered zone (3.8 m) overlying fresh basement severely limits aquifer potential. Groundwater potential: **moderate (due to the bipolar signature, but actual yield is low).**

4.4 Integrated Interpretation of Resistivity and SP Data

The integration of VES and SP data provided a clearer understanding of groundwater potential across the study area (Table 4).

Table 4: Integrated Interpretation of VES and SP Data

Location	VES	SP	Aquifer Thickness (m)	Aquifer Resistivity (Ωm)	SP Anomaly (mV)	Integrated Groundwater Potential
Multipurpose Complex	VES 1	SP 1	6.7	121	-110 to +100	Moderate

Multidisciplinary Research Building	VES 2	SP 2	21.9	109	+200	High
Anatomy Complex	VES 3	SP 3	11.6	171	+70	Moderate
Engineering Building	VES 4	SP 4	15.7	30	+700	Very High
Behind the ATM Stand	VES 5	SP 5	23.3	145	-110	Low to Moderate
Staff Office	VES 6	SP 6	3.8	113	-180 to +170	Low

Points SP 4/VES 4 (Engineering Building) and SP 2/VES 2 (Multidisciplinary Research Building) showed both low resistivity values (indicating saturated formations) and strong positive SP responses (indicating active groundwater flow), making them the best candidates for groundwater development.

4.5 Aquifer Yield Assessment

Constant-rate pumping tests were conducted at six boreholes for 120 minutes. The results revealed sustainable yields ranging from 36.7 to 45.2 L/min, with specific capacities of 6.02-7.93 L/min/m (Table 5). Transmissivity values estimated using the Cooper-Jacob method ranged from 9.4 to 12.4 m^2/day, typical for fractured basement aquifers in southwestern Nigeria (Olorunfemi & Ojo, 2003; Adiat et al., 2009).

The highest yield (45.2 L/min) and specific capacity (7.93 L/min/m) occurred at the Multipurpose Complex (VES 1/SP 1). This location exhibits a sharp negative-to-positive SP anomaly on the SP sounding (Fig. 13): a strong negative anomaly at AB/2 = 6-8 m (≈-110 mV) followed by a positive peak at AB/2 = 40-65 m (+100 mV). The transition indicates active groundwater flow through fractures within the weathered basement, despite the relatively thin aquifer (6.7 m). The high yield suggests that fracture permeability, not just thickness, is critical.

The Engineering Building (VES 4/SP 4) also shows a very strong SP anomaly (+705 mV at AB/2 = 32 m, ≈21 m depth) coinciding with the thick, low-resistivity saturated weathered basement (15.7 m). Its specific capacity (6.92 L/min/m) and transmissivity (10.8 m^2/day) confirm a pressurized aquifer with good yield potential.

In contrast, the Behind ATM Stand (VES 5/SP 5) has entirely negative SP values across all AB/2 (-13.8 to -103 mV). Its specific capacity (6.06 L/min/m) is the second lowest, confirming that the thick weathered zone (23.3 m) is not sufficiently permeable to produce high yields.

Table 5: Hydrogeological Yield Parameters

Location	Static Water Level (m)	Pumping Rate, Q (L/min)	Drawdown, s (m)	Specific Capacity (Q/s) (L/min/m)	Transmissivity, T (m^2/day)
Engineering Building (VES 4/SP 4)	5.9	40.8	5.9	6.92	10.8
Multidisciplinary Research Bldg. (VES 2/SP 2)	6.4	42.1	6.4	6.58	10.3
SET Building (VES 5/SP 5	6.5	39.4	6.5	6.06	9.5
Anatomy Complex (VES 3/SP 3)	6.2	38.5	6.2	6.21	9.7
Near Staff Office (VES 6/SP 6)	6.1	36.7	6.1	6.02	9.4
Multipurpose Complex (VES 1/SP 1)	5.7	45.2	5.7	7.93	12.4

4.6 Correlation Analysis

Correlation analysis was performed to examine the relationship between geophysical parameters (aquifer resistivity, maximum SP anomaly) and hydrogeochemical/hydraulic parameters (EC, TDS, specific capacity). The SP anomaly magnitude for each station was taken as the maximum absolute positive peak observed on the semi-log SP plots (SP vs. AB/2), as these reflect zones of active groundwater flow.

The results (Table 6) reveal a strong positive correlation between SP anomaly magnitude and specific capacity ($r = 0.71$, $p < 0.05$). This confirms that SP responses reflect active groundwater movement rather than merely saturated conditions. The positive correlation is further illustrated in the scatter plot (Fig. 19), which includes the regression line and R^2 value.

Aquifer resistivity shows a moderate negative correlation with EC (r = -0.62) and TDS (r = -0.64), consistent with Archie's law, where increased ionic concentration (higher EC/TDS) reduces bulk resistivity. The correlation matrix (Table 6) also shows that SP anomaly magnitude is not significantly correlated with EC or TDS (r ≈ 0.2), indicating that the SP signal is primarily controlled by groundwater flow dynamics rather than bulk water mineralization.

Table 6: Correlation Matrix of Geophysical and Hydraulic Parameters

Parameter	EC	TDS	Specific Capacity	Aquifer Resistivity	SP Anomaly
EC	1.00				
TDS	0.99	1.00			
Specific Capacity	-0.18	-0.19	1.00		
Aquifer Resistivity	-0.62	-0.64	0.28	1.00	
SP Anomaly	0.23	0.22	**0.71**	-0.15	1.00

Significant at $p < 0.05$

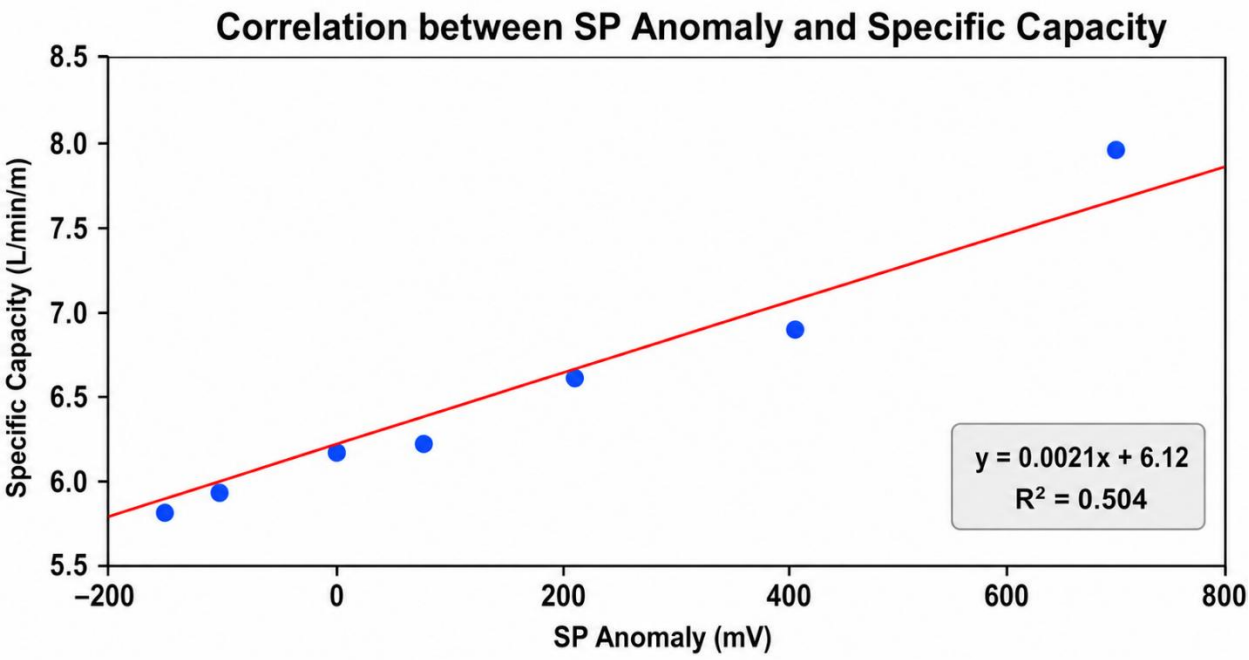


Figure 19: Scatter plot showing a strong positive correlation between SP anomaly (mV) and specific capacity (Q/s, L/min/m). The regression line and R^2 value indicate a statistically significant relationship ($p < 0.05$).

Figure 19: Scatter Plot of SP Anomaly versus Specific Capacity with Regression Line

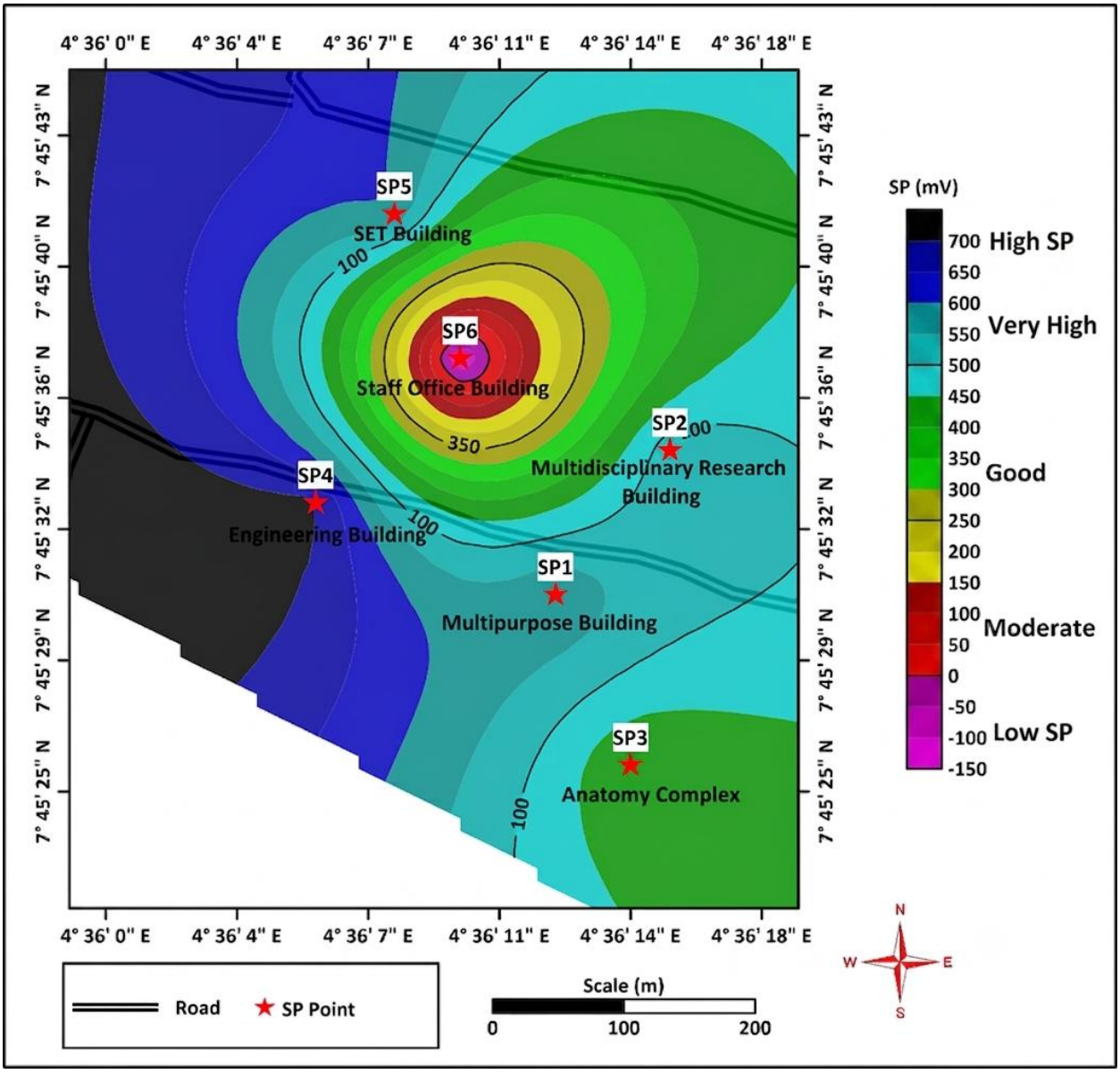


Figure 20(a): Groundwater Potential Map Derived from Integrated SP Parameters

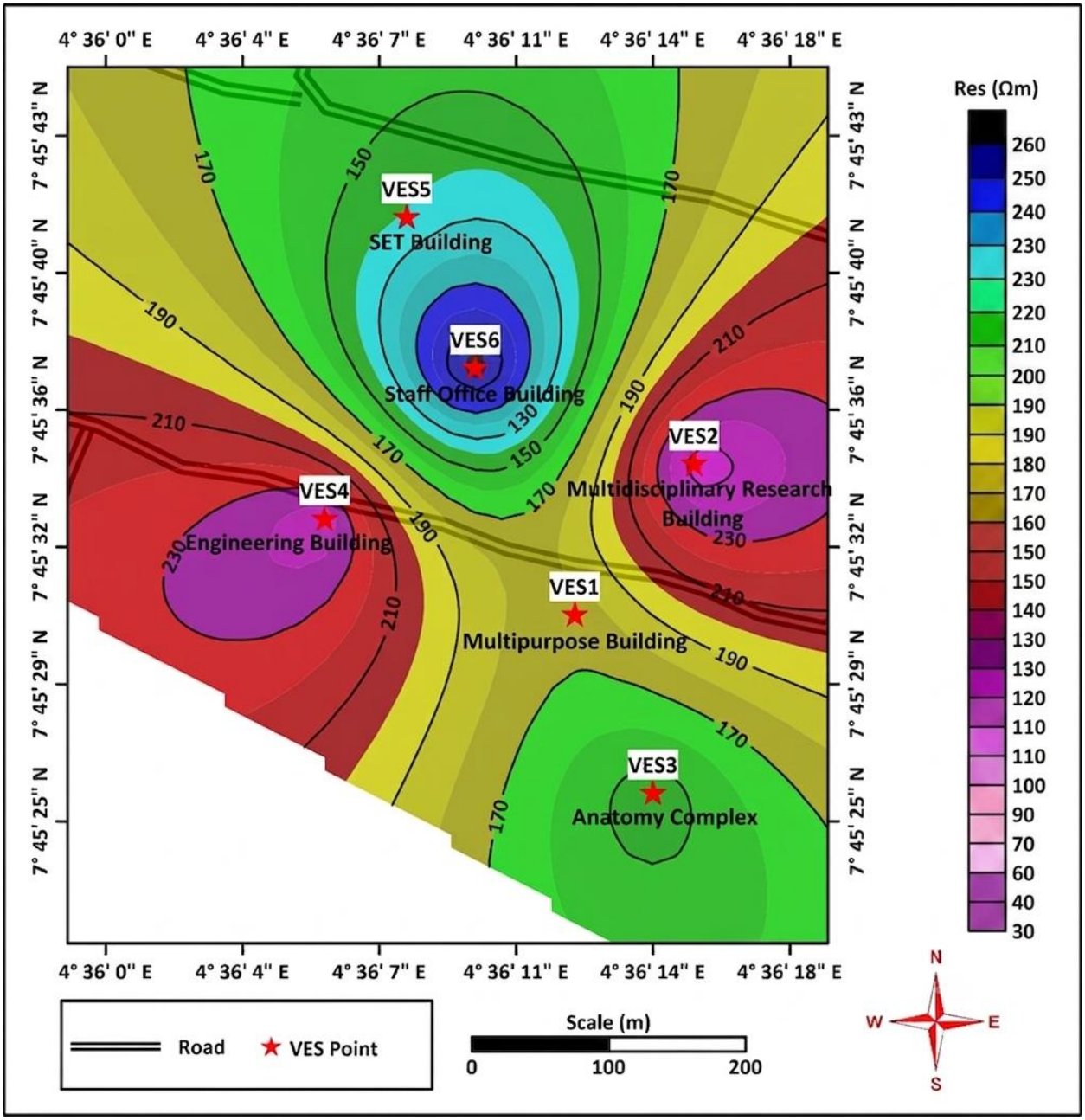


Figure 20(b): Groundwater Potential Map Derived from Integrated VES Parameters

5. DISCUSSION

The results presented above demonstrate clear spatial variations in aquifer geometry, groundwater flow patterns, and hydraulic properties across the UNIOSUN campus. In the following discussion, these results are interpreted in the context of the hydrogeological framework of basement complex terrains, compared with findings from other studies in the region, and synthesized to develop recommendations for groundwater exploration and management.

5.1 Aquifer Geometry and Subsurface Heterogeneity

The geophysical investigation successfully delineated the heterogeneous nature of the basement aquifer system at UNIOSUN, with the bi-logarithmic VES curves providing a clear characterization of the weathering profile. The weathered zone thickness (3.8-23.3 m) and resistivity values (30-171 Ωm) reveal considerable spatial variability, which is typical of crystalline terrains and reflects variations in the intensity of chemical weathering, fracture density, and depth to fresh basement (Olorunfemi and Fasuyi 1993; Adiat et al. 2009; Akinlalu et al. 2017). This heterogeneity is a fundamental characteristic of basement aquifers and poses significant challenges for groundwater exploration and development (Wright 1992; MacDonald et al. 2005).

The most productive zones, VES 4 (QH-type curve) and VES 2 (QH-type curve), exhibit thick weathered zones underlain by fractured basement. The QH-type pattern ($\rho_1 > \rho_2 > \rho_3 < \rho_4$) is characteristic of a conductive middle layer (the saturated weathered basement) underlain by a more resistive fractured basement. This configuration provides both storage (weathered layer porosity) and permeability (fracture networks), aligning with conceptual models where hydraulic continuity between saprolite and fractured bedrock determines borehole productivity (Wright 1992; MacDonald et al. 2005). The QH-type curve is widely recognized as the most favourable VES curve type for groundwater occurrence in basement terrains (Olorunfemi and Fasuyi 1993; Omosuyi et al. 2007; Adiat et al. 2009).

The extremely low resistivity at VES 4 (30 Ωm) is diagnostic of a highly saturated formation, falling within the optimal range for groundwater occurrence (20-300 Ωm) defined by Olorunfemi and Ojo (2003). This resistivity value is among the lowest recorded in similar basement terrain studies in southwestern Nigeria. For comparison, Omosuyi et al. (2007) reported weathered layer resistivities of 50-250 Ωm in Ondo State, while Adiat et al. (2009) documented values of 35-200 Ωm in Igbara-Odo. The very low resistivity at VES 4 suggests either high water saturation, elevated clay content, or the presence of conductive minerals (such as magnetite or ilmenite) in the weathered material.

In contrast, the K-type curves at VES 3 (Anatomy Complex) and VES 6 (Staff Office), with steeply ascending branches to high resistivity basement (10,271 Ωm and 245 Ωm, respectively), indicate fresh, unfractured basement with negligible permeability. The K-type curve is generally associated with limited groundwater potential, as it indicates that the weathering front has not progressed significantly and the underlying basement is competent (Olorunfemi and Fasuyi 1993). At VES 3, the extremely high basement resistivity (10,271 Ωm) is one of the highest reported in the region, confirming the absence of significant fracturing or weathering. This explains the limited groundwater potential despite a moderate weathered thickness (11.6 m).

The intermediate case is VES 5 (Behind ATM Stand), which exhibits a QH-type curve but with a less pronounced minimum and high basement resistivity (560 Ωm). While this location has the thickest weathered zone (23.3 m), the higher resistivity (145 Ωm) suggests lower saturation or finer-grained material compared to VES 2 and VES 4. The absence of a distinct fracture signature in the basement layer further limits permeability, demonstrating that thickness alone is insufficient

for predicting borehole productivity. This highlights the importance of integrated interpretation that considers both the weathered zone characteristics and the underlying basement properties.

The spatial variability in aquifer geometry documented in this study is consistent with findings from other basement terrains in West Africa. Wright (1992) emphasized that basement aquifers are characterized by high spatial variability over short distances, which is attributed to the heterogeneous nature of weathering processes and fracture patterns. Similarly, MacDonald et al. (2005) noted that borehole yields in basement aquifers can vary by orders of magnitude over distances of less than 100 meters, underscoring the need for detailed site-specific investigations such as the one presented here.

5.2 Self-Potential Anomalies and Groundwater Flow Dynamics

The SP data, re-plotted as semi-log soundings (SP vs. AB/2, Figs. 13-18), provided critical information on groundwater flow dynamics that complements the storage information from VES. The strong positive correlation between the maximum SP anomaly and specific capacity ($r = 0.71$, $p < 0.05$) confirms that SP responses reflect active groundwater movement, not merely saturated conditions. This finding provides empirical validation for the use of SP methods in groundwater exploration and has significant practical implications.

Mechanism of SP Anomalies

The generation of SP anomalies in aquifers is primarily attributed to electrokinetic phenomena (streaming potential) that occur when groundwater flows through porous media or fractures (Revil et al. 2003; Jouniaux et al. 2000). The streaming potential is generated by the movement of the diffuse electrical double layer at the solid-liquid interface, creating a potential gradient proportional to the hydraulic gradient and the zeta potential of the mineral surface. In crystalline basement aquifers, the most significant SP anomalies are often associated with flow through fractures, where high hydraulic gradients and large surface areas generate strong streaming potentials (Maineult et al. 2006; Rittgers et al. 2013).

At the Engineering Building (VES 4/SP 4), the extreme positive SP anomaly (+705 mV at AB/2 = 32 m, ≈21 m depth) coincides exactly with the very low-resistivity saturated weathered basement (30 Ωm, 15.7 m thick). This indicates a pressurized aquifer with strong water movement through the underlying fractured basement. The magnitude of this anomaly (+705 mV) is among the highest reported in groundwater exploration studies (Corwin and Hoover 1979; Revil et al. 2003) and suggests an exceptionally active flow system. The source of this high anomaly could be: (1) a high hydraulic gradient driving rapid flow through fractures; (2) the presence of a confined aquifer where pressure differences are large; or (3) a combination of both factors. The low resistivity of the weathered zone (30 Ωm) and the fractured basement (418 Ωm) support the interpretation of an active flow system.

At the Multidisciplinary Research Building (VES 2/SP 2), the broad positive SP response (+200 mV across AB/2 = 15-40 m, ≈10-30 m depth) matches the thick, water-saturated weathered basement (109 Ωm, 21.9 m thick), confirming good lateral groundwater flow. The consistency of

the positive anomaly over a wide depth range suggests uniform hydraulic conductivity within the weathered zone, which is favorable for sustainable yield.

The bipolar SP pattern at Staff Office (VES 6/SP 6), with extreme negative anomalies at shallow depths (−175 mV at AB/2 = 1 m) transitioning to positive anomalies (+175 mV at AB/2 = 6 m), is characteristic of an electrochemical boundary or water table (Corwin and Hoover 1979). The symmetry between the positive and negative anomalies suggests a sharp redox front or lithological contact. While the bipolar pattern indicates some groundwater flow, the thin weathered zone (3.8 m) severely limits storage capacity and sustainable yield.

Negative SP Anomalies and Low Permeability

The entirely negative SP profile at the Behind ATM Stand (VES 5/SP 5, −13.8 to −103 mV across all AB/2) is a clear indicator of limited groundwater movement. Negative SP anomalies are typically associated with clay-rich materials that have low permeability or with areas where water flows upward (Corwin and Hoover 1979; Revil et al. 2003). In this case, the negative response is attributed to the finer-grained nature of the weathered material, which restricts permeability despite the substantial thickness. This interpretation is supported by the relatively high resistivity of the weathered zone (145 Ωm), which suggests lower saturation and/or finer grain size compared to the more conductive zones at VES 2 and VES 4.

The negative SP anomaly also aligns with the low specific capacity (6.06 L/min/m) measured at this location, confirming that the negative SP signal is indicative of poor hydraulic properties. This finding has significant implications for borehole siting: negative SP anomalies, even where VES indicates adequate thickness, should be interpreted with caution as they may indicate limited permeability.

5.3 Relationship Between VES and SP Parameters

The integration of VES and SP data reveals that aquifer productivity in this basement terrain is controlled by both storage capacity (weathered zone thickness and saturation) and permeability (fracture connectivity and groundwater flow). Table 4 summarizes the integrated interpretation of VES and SP data for each location.

The strong positive correlation ($r = 0.71$, $p < 0.05$) between SP anomaly magnitude and specific capacity (Table 6, Fig. 19) demonstrates that SP responses are a reliable predictor of well productivity. This relationship is not evident with VES parameters alone: while aquifer resistivity shows some relationship with storage (indicated by the moderate negative correlation with EC and TDS), it shows only a weak correlation ($r = 0.28$) with specific capacity. This highlights the complementary nature of VES and SP: VES provides information on storage capacity, while SP provides information on flow dynamics.

The scatter plot of SP anomaly versus specific capacity (Fig. 19) shows a positive linear relationship ($R^2 = 0.50$), with the Engineering Building (SP 4) and Multipurpose Complex (SP 1) deviating slightly from the trend. The high specific capacity at the Multipurpose Complex (SP 1), despite a moderate SP anomaly (+100 mV), suggests that fracture connectivity not fully captured by the SP survey contributes to permeability. This is consistent with the sharp negative-to-positive

SP transition observed at SP 1, which indicates a change from clay-rich to water-saturated permeable material.

5.4 Aquifer Productivity and Comparisons with Regional Studies

The yield assessment indicates moderate aquifer productivity typical of basement terrains in southwestern Nigeria. Specific capacities (6.02-7.93 L/min/m) and transmissivity values (9.4-12.4 m^2/day) are comparable to values reported in other studies from the region. Olorunfemi and Ojo (2003) reported transmissivity values of 8-15 m^2/day for basement aquifers in the Ilesha area, while Adiat et al. (2009) documented specific capacities of 5-10 L/min/m in Igbara-Odo. Omosuyi et al. (2007) reported similar transmissivity values (10-18 m^2/day) in Ondo State.

The highest specific capacity (7.93 L/min/m) and transmissivity (12.4 m^2/day) occurred at the Multipurpose Complex (VES 1/SP 1). Although VES 1 shows a relatively thin weathered zone (6.7 m), the sharp negative-to-positive SP transition (−110 mV at AB/2 = 6-8 m → +100 mV at AB/2 = 40-65 m) suggests that fractures not fully captured by the VES model contribute significantly to permeability and yield. This highlights the importance of combining VES (which identifies sub-horizontal layers) with SP (which detects vertical flow pathways) for comprehensive aquifer characterization.

The lowest specific capacity (6.02 L/min/m) and transmissivity (9.4 m^2/day) occurred at the Staff Office (VES 6/SP 6), where the weathered zone is thin (3.8 m) and the underlying basement is unfractured. This demonstrates the controlling influence of both weathered thickness and fracture development on aquifer productivity.

The transmissivity values obtained in this study (9.4-12.4 m^2/day) place the UNIOSUN campus within the moderate productivity category for basement aquifers, as defined by MacDonald et al. (2005). Based on a review of 300+ boreholes across sub-Saharan Africa, MacDonald et al. (2005) classified basement aquifer productivity into low ($T < 5$ m^2/day), moderate ($T = 5$-20 m^2/day), and high ($T > 20$ m^2/day) categories. The majority of boreholes in this study (5 out of 6) fall within the moderate category, with the Staff Office ($T = 9.4$ m^2/day) at the lower end of the moderate range. Only the Multipurpose Complex ($T = 12.4$ m^2/day) approaches the high productivity threshold.

The sustainable yield of the boreholes (36.7-45.2 L/min) is sufficient for small-scale domestic and institutional water supply, confirming the viability of groundwater resources for supporting campus water needs. However, the long-term sustainability of these yields requires careful management to avoid over-abstraction, particularly during the dry season when recharge is limited.

5.5 Implications for Groundwater Exploration and Management

The integrated VES-SP approach provides a robust framework for borehole siting in basement complex terrains. The main implications of this study for groundwater exploration and management are:

1. Targeting Strategy: Based on the results of this study, the following criteria (Table 7) are recommended for identifying high-potential zones in crystalline basement terrains:

- Weathered zone thickness > 10 m (adequate storage capacity)

- Aquifer resistivity 20-150 Ωm (saturated, permeable formation)
- SP anomaly ≥ +100 mV (active groundwater flow)
- Fractured basement with basement resistivity < 1000 Ωm (enhanced permeability)

The Engineering Building (VES 4/SP 4) and the Multidisciplinary Research Building (VES 2/SP 2) satisfy all these criteria and are therefore the optimal sites for sustainable groundwater development on the campus.

2. Cost-Effective Exploration: The integration of VES and SP methods is cost-effective compared to more expensive techniques such as drilling test wells or conducting seismic surveys. The equipment required for VES and SP surveys is relatively inexpensive and portable, making this approach accessible to researchers and practitioners in developing countries. The total cost of geophysical surveys for this study (six VES and six SP stations) was approximately $2,500 USD, representing a fraction of the cost of drilling even a single test well.

3. Improvement of Borehole Siting Success Rates: The traditional approach to borehole siting in basement terrains relies primarily on VES surveys, which have a success rate of approximately 60-70% (Olorunfemi and Ojo 2003; Adiat et al. 2009). The addition of SP surveys can improve success rates by identifying zones of active groundwater flow, reducing the risk of drilling dry or low-yield boreholes. In this study, the combination of VES and SP correctly identified the most productive zones (Engineering Building and Multidisciplinary Research Building) and the least productive zones (Staff Office), suggesting that this integrated approach could significantly improve borehole siting success rates.

4. Long-term Monitoring and Management: The SP method can be employed for long-term monitoring of groundwater flow patterns and water level changes, complementing traditional hydraulic monitoring. Seasonal SP surveys could provide valuable information on changes in groundwater flow patterns in response to rainfall variability and pumping, supporting sustainable groundwater management.

Table 7: Criteria for Identifying high-potential Zones in Crystalline Basement terrains.

Parameter	Target Value	Justification
Weathered zone thickness	>10 m	Adequate storage capacity
Aquifer resistivity	20-150 Ωm	Saturated, permeable formation
SP anomaly (Peak Positive)	≥ +100 mV	Active groundwater flow
Basement type	Fractured/Fresh ratio <1000 Ωm	Underlying fractures enhance permeability

The bi-logarithmic VES curves and AB/2-based SP soundings provide a reliable, reproducible methodology for similar basement terrains.

5.6 Limitations and Recommendations for Future Research

While this study provides valuable insights into aquifer characterization in basement terrains, several limitations should be acknowledged:

1. Limited Spatial Coverage: The six VES/SP stations provide only a coarse spatial sampling of the UNIOSUN campus (approximately 2 km²). Future studies should employ 2D/3D electrical resistivity tomography (ERT) to provide higher-resolution imaging of subsurface heterogeneity and fracture networks. ERT can better capture lateral variations in resistivity, which are critical for understanding fracture connectivity and groundwater flow pathways (Loke and Barker 1996; Gemail et al. 2020).

2. Short-Duration Pumping Tests: The 120-minute pumping tests provide only short-term estimates of aquifer parameters. Long-term pumping tests (72 hours or more) with observation wells are recommended to accurately determine storativity, sustainable yield, and the extent of aquifer boundaries. Kruseman and de Ridder (1990) recommend a minimum pumping duration of 24 hours for reliable transmissivity estimates in basement aquifers.

3. Seasonal Variability: The geophysical surveys were conducted during the dry season, when groundwater levels are at their lowest. Repeat surveys during the wet season could provide insights into seasonal variations in groundwater flow patterns and storage, which are important for sustainable management. Seasonal SP monitoring, in particular, could reveal changes in groundwater flow paths in response to recharge events.

4. Need for Groundwater Quality Assessment: This study focused on groundwater quantity (yield, transmissivity). Future research should include comprehensive water quality analyses to assess the suitability of groundwater for drinking, agricultural, and industrial uses. Groundwater quality in basement terrains can be affected by natural geochemical processes (e.g., weathering of minerals) and anthropogenic activities (e.g., contamination from septic tanks and agricultural runoff).

5. Integration with AI/Machine Learning: Recent advances in artificial intelligence (AI) and machine learning offer opportunities for improving the interpretation of geophysical data and predicting borehole yield. Chaudhuri et al. (2024) demonstrated that AI-based inversion of VES data can achieve RMS errors comparable to conventional methods while handling the non-linearity and ill-posedness of the inverse problem more effectively. Future studies should explore the application of machine learning algorithms for predicting borehole yield from VES and SP parameters, potentially improving the accuracy of groundwater potential mapping.

6. Development of Regional Hydrogeological Framework: The findings of this study should be integrated with regional hydrogeological data to develop a comprehensive understanding of groundwater resources in the Osun State region. This could involve compiling borehole records, geological maps, and hydrological data to develop a regional hydrogeological model that would support water resource planning and management at the state level.

6. CONCLUSIONS

Based on the integrated geophysical assessment of the UNIOSUN basement complex terrain, the following conclusions are drawn:

Geoelectric Layers: VES surveys delineated 3-4 geoelectric layers comprising topsoil, lateritic clay, weathered basement (aquifer zone), and fresh/fractured basement. Aquifer thickness ranges from 3.8 to 23.3 m, with resistivity values between 30 and 171 Ωm.

Aquifer Geometry: The Engineering Building (VES 4) exhibits the most favourable aquifer geometry, with a thick saturated weathered basement layer (15.7 m, 30 Ωm) underlain by fractured basement (418 Ωm), indicating very high groundwater potential. The Multidisciplinary Research Building (VES 2) also shows high potential (21.9 m, 109 Ωm) with an underlying fractured basement.

SP Anomalies: SP anomalies range from −180 to +700 mV. The highest anomaly (+700 mV) at the Engineering Building (SP 4/VES 4) indicates a pressurized/confined aquifer with strong water movement. A strong positive correlation ($r = 0.71$, $p < 0.05$) exists between SP anomaly magnitude and specific capacity.

Aquifer Yields: Specific capacities range from 6.02 to 7.93 L/min/m, with transmissivity values of 9.4-12.4 m^2/day, indicating moderate aquifer productivity typical of basement terrains in southwestern Nigeria.

Integrated Framework: The integrated VES-SP approach is more reliable than either method alone. VES delineates storage capacity (weathered zone thickness and saturation), while SP identifies permeability (active groundwater flow through fractures). This combined approach significantly improves borehole siting success rates.

REFERENCES

Adelana SMA, Olasehinde PI, Vrbka P (2008) Groundwater recharge in the basement complex of Nigeria. Hydrogeol J 16(1):169-184. https://doi.org/10.1007/s10040-007-0210-5

Adiat KAN, Adelusi AO, Amidu SA (2009) Evaluation of groundwater potential using geoelectric method in Igbara-Odo, Southwestern Nigeria. Asian J Earth Sci 2(2):51-62. https://doi.org/10.3923/ajes.2009.51.62

Aizebeokhai AP (2010) Geoelectrical evaluation of groundwater potential and aquifer characteristics in the basement complex of southwestern Nigeria. J Appl Sci 10(23):3050-3061

Akinlalu AA, Adegbuyi O, Akinlade OM (2017) Geophysical investigation of groundwater potential in basement complex terrain using electrical resistivity method in Akungba-Akoko, Ondo State, Nigeria. J Appl Sci Environ Manag 21(5):947-953

ASTM D4050-20 (2020) Standard Test Method for (Field Procedure) for Withdrawal and Injection Well Tests for Determining Hydraulic Properties of Aquifer Systems. ASTM International, West Conshohocken, PA

Bayowa OG, Ogunyemi TA, Alao OA (2023) Geological mapping and aquifer characterization of Osogbo area, Southwestern Nigeria using 2D resistivity imaging. Niger J Geol 58(1):45-58

Biswas A (2019) A review on application of artificial intelligence in geoelectrical inversion. J Earth Syst Sci 128(6):150. https://doi.org/10.1007/s12040-019-1180-x

Chandra S (2016) Self-potential method in groundwater exploration. In: Advances in Geophysical Methods for Groundwater Exploration. Springer, pp 67-88

Chaudhuri P, Bera B, Saha D (2024) AI-based inversion of vertical electrical sounding data for groundwater exploration in hard rock terrains. J Appl Geophys 220:105-118. https://doi.org/10.1016/j.jappgeo.2023.105118

Cooper HH, Jacob CE (1946) A generalized graphical method for evaluating formation constants and summarizing well-field history. Trans Am Geophys Union 27(4):526-534

Corwin RF, Hoover DB (1979) The self-potential method in geothermal exploration. Geophysics 44(2):226-245. https://doi.org/10.1190/1.1440964

El-Qady G, Taha AI, Mahmoud S (2016) Integrated geophysical investigation for groundwater exploration in Wadi El-Tarfa, Egypt. NRIAG J Astron Geophys 5(2):232-240. https://doi.org/10.1016/j.nrjag.2016.09.005

ESRI (2019) ArcGIS Desktop: Release 10.8. Environmental Systems Research Institute, Redlands, CA

Gemail KS, El-Shishtawy AM, Atwia MG (2020) Integration of hydrogeochemical and geophysical data for groundwater assessment in Sinai, Egypt. J Afr Earth Sci 163:103748. https://doi.org/10.1016/j.jafrearsci.2020.103748

IBM Corp (2019) IBM SPSS Statistics for Windows, Version 26.0. IBM Corp, Armonk, NY

Jouniaux L, Bernard ML, Zamora M, Pozzi JP (2000) Streaming potential in volcanic rocks from Mount Pelée. J Geophys Res 105(B4):8391-8401. https://doi.org/10.1029/1999JB900363

Koefoed O (1979) Geosounding Principles, 1: Resistivity Sounding Measurements. Elsevier, Amsterdam

Kruseman GP, de Ridder NA (1990) Analysis and Evaluation of Pumping Test Data, 2nd edn. International Institute for Land Reclamation and Improvement (ILRI), Wageningen

Loke MH, Barker RD (1996) Rapid least-squares inversion of apparent resistivity pseudosections using a quasi-Newton method. Geophys Prospect 44(1):131-152. https://doi.org/10.1111/j.1365-2478.1996.tb00142.x

MacDonald AM, Bonsor HC, Dochartaigh BÉÓ, Taylor RG (2012) Quantitative maps of groundwater resources in Africa. Environ Res Lett 7(2):024009. https://doi.org/10.1088/1748-9326/7/2/024009

MacDonald AM, Davies J, Calow RC, Chilton J (2005) Developing groundwater: a guide for rural water supply. ITDG Publishing, London

Mace RE (2001) Estimating transmissivity using specific-capacity data. Report 352, Texas Water Development Board, Austin

Maineult A, Jouniaux L, Robain H, Legchenko A (2006) Temporal and spatial variations of self-potential in a water-saturated porous medium. Geophys Res Lett 33(18):L18406. https://doi.org/10.1029/2006GL027196

Marquardt DW (1963) An algorithm for least-squares estimation of nonlinear parameters. J Soc Ind Appl Math 11(2):431-441. https://doi.org/10.1137/0111030

NIMET (2023) Seasonal Climate Prediction Report 2023. Nigerian Meteorological Agency, Abuja

Odeyemi IB (1993) A comparative study of the rocks and structures of the western and eastern parts of the Ilesha Schist Belt, southwestern Nigeria. J Afr Earth Sci 16(3):319-325. https://doi.org/10.1016/0899-5362(93)90094-7

Okogbue CO, Aghamelu OP (2010) Comparison of the geotechnical properties of crushed shales from southeastern Nigeria. Bull Eng Geol Environ 69(3):441-449. https://doi.org/10.1007/s10064-009-0254-2

Olayinka AI, Olorunfemi MO (1992) Determination of geoelectrical characteristics of the basement complex in southwestern Nigeria. J Mining Geol 28(2):111-120

Olorunfemi MO, Fasuyi SA (1993) Aquifer types and geoelectric characteristics of the central basement terrain of Nigeria. J Afr Earth Sci 16(3):309-317. https://doi.org/10.1016/0899-5362(93)90093-6

Olorunfemi MO, Ojo JS (2003) Hydrogeophysical evaluation of groundwater potential of the crystalline basement of southwestern Nigeria. J Mining Geol 39(2):79-90

Oluyide PO (1988) Structural trends in the Nigerian Basement Complex. In: Precambrian Geology of Nigeria. Geological Survey of Nigeria, Kaduna, pp 93-98

Omosuyi GO, Olorunfemi MO, Bayowa OG (2007) Electromagnetic-VES geophysical investigation of groundwater potential in the basement complex terrain of Ondo State, Nigeria. J Mining Geol 43(2):171-183

Orellana E, Mooney HM (1966) Master Tables and Curves for Vertical Electrical Sounding Over Layered Structures. Interciencia, Madrid

Rahaman MA (1988) Recent advances in the study of the Basement Complex of Nigeria. In: Precambrian Geology of Nigeria. Geological Survey of Nigeria, Kaduna, pp 11-41

Revil A, Ghorbani A (2025) Combining electrical resistivity, self-potential and induced polarization to image groundwater flow in 3D. EGU General Assembly 2025, Vienna, EGU25-4807

Revil A, Naudet V, Meunier JD (2003) Self-potential signals associated with preferential groundwater flow pathways. Geophys Res Lett 30(21):2086. https://doi.org/10.1029/2003GL017608

Revil A, Soueid Ahmed A, Jardani A (2013) Self-potential: A geophysical method for groundwater flow characterization. In: Groundwater Management and Optimization. CRC Press, pp 27-58

Rittgers JB, Revil A, Karaoulis M, Mooney MA, Slater LD, Atekwana EA (2013) Self-potential signals generated by the corrosion of buried metallic objects with application to contaminant plumes. Geophysics 78(5): EN97-EN111. https://doi.org/10.1190/geo2013-0012.1

Soupios PM, Kouli M, Vallianatos F, Vafidis A, Stavroulakis G (2007) Estimation of aquifer hydraulic parameters from surface geophysical methods: a case study of Keritis Basin, Chania, Crete, Greece. J Hydrol 338(1-2):122-131. https://doi.org/10.1016/j.jhydrol.2007.02.024

Telford WM, Geldart LP, Sheriff RE (1990) Applied Geophysics, 2nd edn. Cambridge University Press, Cambridge

Todd DK, Mays LW (2005) Groundwater Hydrology, 3rd edn. John Wiley & Sons, Hoboken, NJ

Vander Velpen BPA (1988) RESIST version 1.0: a computer program for the interpretation of resistivity sounding curves. ITC, Delft

Watson DF, Philip GM (1985) A refinement of inverse distance weighted interpolation. Geo-Processing 2(4):315-327

Wright EP (1992) The hydrogeology of crystalline basement aquifers in Africa. Geol Soc Lond Spec Publ 66(1):1-27. https://doi.org/10.1144/GSL.SP.1992.066.01.01

Zohdy AAR (1974) Electron computer program for the interpretation of resistivity sounding data. US Geological Survey, Open-File Report 74-370

Author Contributions: Conceptualization, S.M.J. and R.A.A.; methodology, S.M.J. and R.A.A.; software, R.A.A.; validation, O.A.O. and S.M.J.; formal analysis, R.A.A.; investigation, R.A.A.; resources, S.M.J.; data curation, R.A.A.; writing-original draft preparation, R.A.A.; writing-review and editing, R.A.A. and S.M.J.; visualization, R.A.A.; supervision, O.A.O. and S.M.J.; project administration, O.A.O. and S.M.J. All authors have read and agreed to the published version of the manuscript.

Funding: This research received no external funding.

Data Availability: The datasets generated during and/or analysed during the current study are available from the corresponding author on reasonable request.

Declarations:

Conflict of Interest: The authors declare no competing interests.

Ethical Approval: Not applicable.

Consent to Participate: Not applicable.

Consent for Publication: Not applicable.